1 **Bio-derived lactones – Combustion and exhaust emissions of a new class of renewable**

2 **fuels**

3

4 **Authors: James Frost[a*], Dr Paul Hellier[a], Professor Nicos Ladommatos[a]**

5 [a]Department of Mechanical Engineering, University College London, London WC1E 6BT, U.K

6

7 ***Corresponding author:** Department of Mechanical Engineering, University College London,

8 London WC1E 6BT, U.K. Telephone +447858393022. Email: ucemjfr@ucl.ac.uk

9

10

11

12

13

14

15

16

17

18

19

20

21

22

23

24

25

26

27

28

Abstract

The use of bioderived drop-in fuels is an essential step in the reduction in fossil fuel usage. While ethanol and biodiesel are known quantities, the use of novel biomass that does not compete with food for its production could be vital in ensuring a reliable supply. Lactones are a class of chemicals that can also be sourced from 2nd generation biomass and possess molecular attributes that, from previous investigations within the group, are believed to be effective in reducing particulate emissions relative to diesel, while maintaining high ignition propensity. In this study, a systematic investigation of the combustion and exhaust emissions of a series of lactone fuels in a compression ignition engine was undertaken. The results indicated that blended C6 lactones- ε-caprolactone, δ-hexalactone and γ-caprolactone- displayed promising ignition qualities, relative to butanol, an alcohol often employed in diesel blending experiments. Ignition delay decreased as the length of the lactone side chain increased, but combustion was seemingly more stable in both ε-caprolactone and γ-caprolactone, compared to the methyl branched δ-hexalactone, which possessed the highest CO emissions and particle number. The C10 lactone, γ-decalactone, within the diesel-butanol blend, possessed excellent ignition quality, while also reducing particle mass significantly. All blends produced lower nitrogen oxides (NO_x) emissions and particle mass than unblended fossil diesel. Subsequently, two C10 and two C12 lactones were employed- based on their potential to be derived from biomass- as pure fuels in the diesel engine. Despite significant differences in physical properties compared to diesel, stable combustion was observed, with ignition delay approximately equivalent to that of base diesel. The high carbon number and long alkyl chains of the C12 lactones meant that particulate emissions were comparable to diesel. C10 lactones showed greater alleviation of particulate emissions, likely due to a combination of lower carbon number and extended ignition delay relative to diesel, while all pure lactone fuels significantly reduced NO_x emissions, suggested to be due to combustion phasing.
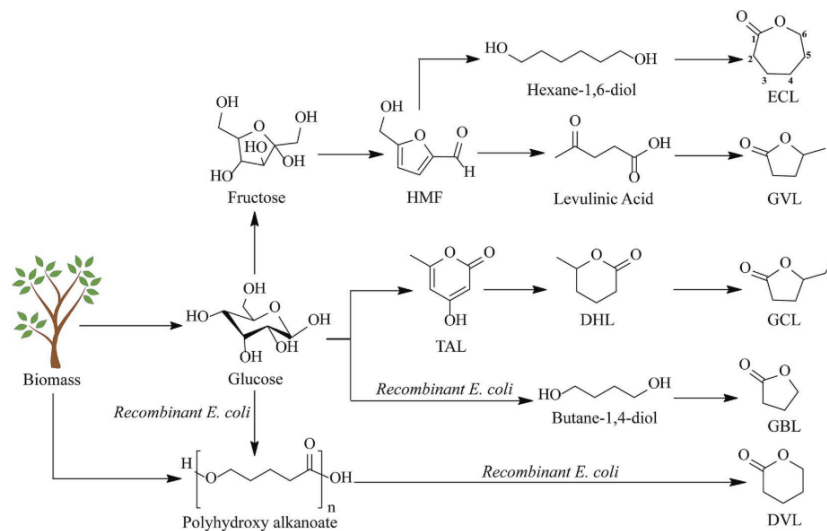
1. Introduction

Crude oil derivatives account for the vast majority of fuels used in the transportation industry; in the US in 2020, approximately 93% of the energy used for transport came from fossil fuels, with only 5% of this energy sourced from biofuels.[1] In the UK, approximately 98% of transportation energy is derived from oil.[2] However, moves away from these petroleum fuels are being made, with a ban on new petrol and diesel cars currently set for 2030 in the UK.[3] The transition period, as well as the fact that cars bought before this ban will likely remain on the road in the 2040s, necessitates the use of cleaner fuels in current internal combustion (IC) engines to mitigate the fossil derived CO_2 emissions produced. However, CO_2 is not the only product of internal combustion. Nitrous oxides (NO_x) and particulate matter/soot (PM) are released as virtually unavoidable by-products of internal combustion of hydrocarbons and both are well-known health hazards.[4–7] Euro 6 limits on NO_x for diesel engines are 0.08g/km and 0.06g/km for petrol engines, with future regulations anticipated to enforce more stringent restrictions still.[8] Catalytic converters are necessary for such low exhaust outputs, but the expense and environmental impact these have in themselves are considerable, while their effectiveness varies considerably with temperature and, therefore, are less effective during engine start-up.[9]

Biofuels could provide a solution to the short to medium-term for combustion engines. Generally containing oxygen within the molecular structure, combustion of these fuels generally result in lower emissions of particulates compared to fossil fuel combustion,[10–12] while production from biomass makes them renewable and potentially carbon-neutral. Today's current fuels contain small amounts of bio-derived components (10% ethanol in gasoline, 7% biodiesel in diesel). However, not only are these relatively low blend ratios, they are also sourced from 1st generation sources i.e those that compete with food sources. Ethanol is often sourced from sugar, while biodiesel from vegetable oils. Research into new types of biodiesel has increased over recent years as cleaner sources of diesel fuel are needed, though their

84   effect on the combustion requires greater understanding and the relative changes in the

85   emissions produced needs clarity.[13–16] Fuels from 2nd generation biomass are a more

86   appealing prospect, as this represents non-edible biomass. Such fuels are derived from

87   lignocellulose; the structure comprising cellulose, hemicellulose and lignin that makes up the

88   basic integrity of all plant life. A previous investigation by the current authors[17] undertook a

89   screening study of various molecules that were deemed to be potentially sourced from this

90   lignocellulose for use diesel blend components. Furfural and hydroxymethylfurfural (HMF) are

91   the main platform chemicals of C5 (hemicellulose) and C6 (cellulose) derived sugars, and thus

92   derivatives of these were used for these tests. The main finding of these experiments was that

93   saturated furans (tetrahydrofurans) were required in diesel engines for high blend ratios to be

94   employed, while maintaining stable combustion. Stable combustion is a loosely defined term

95   in which the coefficient of variation (COV) in the IMEP is low (typically below 10%) and is

96   achieved when ignition occurs at favourable timings close to TDC when the cylinder volume

97   is low and in-cylinder pressures are at their highest. This allows rapid early-stage combustion

98   reactions to ensue, with effective propagation and rapid heat release rates. Furthermore, it

99   was determined that long, single chained alkyl groups were desirable in reducing ignition

100   delay, while the addition of a carbonyl group into the moiety helped reduce particulate mass.

101   The desirable molecular traits described suggest lactones as a bioderived blending

102   component that is both renewable and results in lower toxic emissions. Lactones are cyclic

103   esters, and can vary considerably in their carbon number and ring size. ε-caprolactone (εCL),

104   for example, is a medium size lactones in terms of its ring-size (7 membered ring), and is

105   particularly important due to its current array of uses, as well as its potential to be sourced

106   from lignocellulose (Figure 1.1). Currently however, the major production route utilised for this

107   lactone is through fossil fuels.[18] The biotransformation route to synthesise this lactone is not

108   easily scaled-up, and the demand for ε-caprolactone is extremely high, particularly in the

109   polymer industry (nylon synthesis) with a demand of more than 25,000 tonnes. More recently,

110   εCL production has been developed for 3D printing and for cell culture scaffold purposes.[18]

111   However, there are numerous biopathways available for the production of εCL; cellulose may

112   be dehydrated to produce HMF, which in turn (as investigated by the study of Buntara[19]) can

113   form 1,6-hexanediol through catalytic hydrogenation and hydrodeoxygenation, and

114   subsequently the final lactone product.

115

116   **Figure 1.1: Production routes from 2nd generation biomass to the formation of the C6**

117   **lactones tested[20]**

118

119   Lactones with higher carbon numbers can also be sourced from natural sources and are

120   potentially applicable for diesel blends. Currently, many of these types of molecule are

121   employed in the food, cosmetic and pharmaceutical industries, representing a value of almost

122   US$7 billion a year.[21] γ-decalactone (γDL), for example, has been used as a peach flavouring

123   agent for the food industry in very low levels- possessing a detection threshold of just

124   0.088ppm- and was initially produced directly from fruits or via chemical synthesis.[22] Since γ-

125   decalactone can be classed as a natural food flavouring agent, its bioderived nature is already

126   proven. For the most part, production of this molecule utilises bioconversion of ricinoleic acid,

127   which may be obtained from castor oil. Recently, microbes have been used in the production

128   of this molecule[23] and, while the high cost of this production method is a drawback, Schrader

129   notes that the optimization of the bioconversion of γ-decalactone has contributed to a price

130 drop from $10000/kg to $300/kg.[24] Currently, the price of synthetic 'aroma compounds', such

131 as C10-C12 lactones, are approximately $150/kg, whereas those derived from biologically

132 engineered routes are priced closer to the aforementioned $300/kg value.[25] While currently

133 high, the increased demand for so-called 'natural' flavourings in the food and beverage

134 industry is likely to continue to bring this price down significantly, particularly with the use of

135 enzymes.

136   Gamma lactones in particular are versatile in their use as flavouring agents in foods and

137 cosmetics.[26] From its presence in a wide range of fruits, including apricot, peach, strawberry

138 and mango, and possession of a butter-like[27], the use of γ-dodecalactone (γDDL) in the

139 aforementioned industries has been investigated Hydroxy fatty acids (HFAs) can be used as

140 precursors to the formation of this lactone, though only ricinoleic acid is found in nature in the

141 quantities necessary for large scale application of the lactone.[28] Both 5 member (γ) and 6

142 member (δ) lactones are of interest due to their stability relative to larger and smaller ringed

143 lactones, caused by the minimised bond angle strains for these structures.[29] An isomer of γ-

144 decalactone, δDL differs in that its ring possesses one more carbon atom at the expense of a

145 carbon atom in the side chain. As with the vast majority of long chained lactones, the primary

146 use of this lactone is in fragrances. δ-decalactone itself possesses a cream-coconut and

147 peach aroma.[30] Corma et. al[30] note that a large number of patents have been submitted

148 relating to the production of this molecule, signalling that, irrespective of its potential use as a

149 biofuel, research is already underway into larger scale synthesis. One of the main problems

150 is the use of peracids which involve potentially explosive materials to synthesise and Corma's

151 studies look into the use of more benign (heterogenous) catalysts that remove the need for an

152 organic solvent.[30] However, biological pathways are generally of lower yield than that of the

153 chemical routes- which utilise aldol condensation of cyclopentanone followed by

154 hydrogenation and Baeyer-Villiger oxidation- and therefore have not been scaled up to the

155 same degree.[31] However, Alam et. al report a green synthesis of δDL using the product of

156 fermentation of waste lignocellulosic material, such as sugar cane bagasse, and a one-step

157 hydrogenation reaction in the presence of a heterogeneous catalyst to produce δDL via

158 massoia lactone. Another appealing feature of this synthesis is that the hydrogen required,

159 normally produced from fossil fuels, can be supplied in the form of formic acid, derivable from

160 lignocellulose.[31]

161 A common feature of bio-lactone productions is the use of microbes to allow the

162 transformation of hydroxy fatty acids to the lactone, but a lack of a clear consensus as to which

163 microorganism is most effective, nor where the most likely source of the HFA would be

164 derived, suggests that scale up remains a long-term goal.

165 Examples of the utilisation of lactones as drop-in fuels are scarce. However, one lactone,

166 gamma-valerolactone (GVL), has been tested as a biofuel based on its ability to be derived

167 from 2nd generation biomass; it can be formed from the versatile levulinic acid (LA), which

168 can be obtained from both the cellulose and hemicellulose fraction of biomass components.

169 LA undergoes dehydration to form angelica lactone and is subsequently hydrogenated to form

170 GVL.[32].[33] Bereczky performed the first detailed study of this molecule's combustion in a direct

171 injection, turbocharged diesel engine, referencing the potential advantages in the reduction of

172 emissions to compensate for the low cetane number.[34] Overall, while engine performance was

173 diminished with the addition of biodiesel and GVL, incomplete combustion products, THC and

174 CO, as well as smoke emissions, were significantly reduced, while NO_x emissions were not

175 greatly affected. Due to the size of the GVL molecule, it has been more common to test the

176 lactone in SI engines with higher concentrations than that used in the study of Bereczky (7%).

177 Horvath noted that, compared to ethanol, GVL possesses a similar octane number, but

178 improves combustion due to lower vapour pressure and also has higher energy density

179 compared to ethanol.[35] Furthermore, from a production perspective, GVL is advantageous

180 based on the fact that it does not form an azeotropic mixture with water, which makes the

181 catalyst used in the production both recoverable and reusable, while its high flash point and

182 low toxicity make it a relatively safe molecule to work with.[36] However, in a study by Gschwend

183 looking at 50 alternative fuels, while GVL possessed the basic requirements for an alternative

7

SI engine fuel, the fact that it is also an addictive drug was deemed to render its widespread use unlikely.[37]

For compression ignition engines, a fuel requires greater molecular mass to enhance ignition propensity with a potentially larger radical pool exploited. Larger lactones appear to have received less attention as potential fuels. However, as mentioned, there are promising solutions to the sustainable production of the most commonly utilised of the 'mid-size' lactones; ε-caprolactone. εCL is promising as a fuel blending component when compared to furan molecules that generally possess a lower carbon number (making them more applicable to gasoline blends), while the ester functionality is potentially of benefit in reducing the emission of particulate mass as the number of oxygen atoms available for soot oxidation is increased. ε-caprolactone contains 6 carbon atoms in a cyclic ester structure. Based on the current production potential and higher carbon number of ε-caprolactone compared to GVL (an extensively researched lactone),[34,38,39] The possibility to utilise larger lactones, such as εCL, in diesel engines is therefore highly intriguing. This report is, to the best of our knowledge, the first example of the combustion of higher lactones in a compression ignition engine.

2. Experimental Procedure

2.1. Test molecules

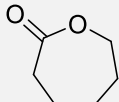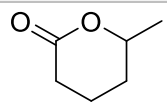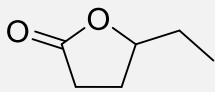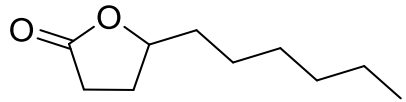The first series of lactones considered, the structures of which are shown in Table 2.1, were used to compare the impact of the ring size and overall carbon number on blending with fossil diesel and the ignition quality. ε-caprolactone (εCL), is a seven membered lactone (six carbons) with no side chains, δ-hexalactone (δHL) also possesses 6 carbons but one of these carbons is branched from a six membered ring, while y-caprolactone (γCL) takes this further by extending the branch to an ethyl chain at the expense of the ring size (five membered).

The comparison of these molecules enabled the impact of the ring size and presence of alkyl chains to be determined while keeping the overall carbon number constant (C6). The fourth lactone tested here, γ-decalactone (γDL), differed by possessing ten carbons (C10).

211   However, as with γ-caprolactone, the cyclic structure consists of four carbons and an oxygen.

212   The purpose of including this molecule was to compare the relative effect of adding further

213   carbons to the chain off the same ring.

214

215   **Table 2.1: Physical properties of three C6 lactones and C10 lactone (γDL) tested in blends**

Molecule	Abbreviation	Structure	Boiling Point (°C)	Density (g/cm^3)*	Viscosity (mPa)* **
ε-caprolactone	εCL		98	1.030	7.44
δ-hexalactone	δHL		111	1.037	4.53
γ-caprolactone	γCL		219	1.023	3.00
γ-decalactone	γDL		281	0.948	7.50
1-Butanol	none		118	0.81	2.53
Diesel	none	N/A	357***	0.834	2.63

216   *at atmospheric temperature

217   **preliminary test results obtained with a Brookfield digital rheometer (Model DV-III)

218   ***final boiling point

219

220   Four lactones were also tested with the prediction of igniting as pure components. The

221   structures and physical properties of these molecules are supplied in Table 2.2 below.
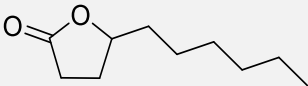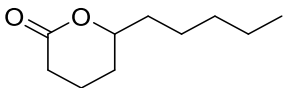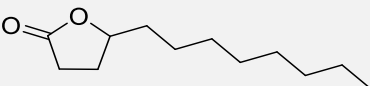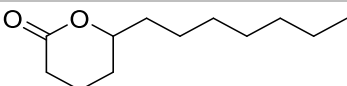
222

223

224

225

226

227

228

229 **Table 2.2: Structures and physical properties of C10 and C12 lactones tested as pure fuels**

Lactone	Abbreviation	Structure	Boiling Point (°C)	Density (g/cm³)*	Viscosity (mPa)* **
γ-decalactone	γDL		281 (760mmHg)	0.948	7.50
δ-decalactone	δDL		283 (760mmHg)	0.954	11.2
γ-dodecalactone	γDDL		130-132 (1.5 mmHg)	0.936	14.6
δ-dodecalactone	δDDL		304 (760mmHg)	0.942	15.0

230 *at atmospheric temperature

231 **preliminary test results obtained with a Brookfield digital rheometer (Model DV-III)*

232

233 ε-caprolactone (>98%), δ-hexalactone (>98%), γ-caprolactone (98%), δ-decalactone (98%),

234 γ-decalactone (>98%), δ-dodecalactone (97%), γ-dodecalactone (>97%). 1-Butanol (99%)

235 was purchased from Alfa Aesar and the zero-FAME fossil diesel used was obtained from

236 Haltermann Carless.

237

238 **2.2. Blending**

239

240   The solubility of the blended lactones (Table 2.1) in fossil diesel fuel varied significantly.

241 To maintain consistency, a constant blend ratio was utilised for all tests which reflected the

242 maximum blend ratio possible for the poorest blending fuel (δHL). Table 2.3 below specifies

243 the volume ratios used for all lactone blends tested. The individual components were

244 measured volumetrically in individual burettes to achieve the desired ratios. A standard

245 sealable glass reagent bottle containing the mixture was initially put onto a magnetic plate,

246 with a magnetic stirrer used for constant agitation of the components as they were added. This

247 was performed for a period of at least 2 minutes after the final component had been added to

248 ensure no phase separation had occurred.

249   Butanol was selected as a co-solvent due to its frequent use in diesel blend studies and

250   the improvement in emissions this molecule can bring when utilised in low quantities.[17,40,41] A

251   study by Yang utilised butanol in a blend with both diesel and GVL, which determined little

252   change in engine power when utilising higher percentages of oxygenated fuel, with major

253   reductions in HC emissions and smoke opacity.[42] In the current study however, the proportion

254   of lactone relative to butanol was maximised so as to best be able to observe the effects of

255   varying lactone molecular structure.

256   εCL was noted to blend poorly with diesel. When diesel was combined in a 50:50 volume

257   ratio with the lactone species, a single-phase solution could not be formed. The size and

258   polarity of a molecule are the main attributes in dictating the solubility of a molecule. Ester

259   molecules tend to be polar and given the rule of 'like- dissolves-like', with diesel being a non-

260   polar solvent, poor blending was not unexpected. The large ring and shape of this molecule

261   are also likely reasons for the poor blending properties in diesel; the ring shape means that it

262   cannot form the necessary Van de Waals forces with diesel molecules, which tend to be long

263   chains of alkanes and alkenes, rendering it poorly soluble.

264   As in the case of ε-caprolactone, δ-hexalactone was noted not to be insoluble in fossil

265   diesel fuel. Moreover, the blending properties were poorer relative to εCL, such that all blend

266   ratios were dictated by δHL solubility. Since the polarity of the various lactones is likely to be

267   very similar, the overall surface area and the orientation in which the diesel molecules may be

268   able to fit around the lactone molecules could explain the observed difference in solubility. The

269   solubility of γCL was found to be higher than that of δ-hexalactone, therefore not following a

270   trend of ring size or side chain length. The longer chain of γCL compared to δHL may present

271   sufficient non-polar sites for diesel molecules to be able to interact to the extent necessary for

272   the lactone to become solvated more effectively than the methyl branched δHL. Compared,

273   however, to εCL to δHL, the former is a more compact structure, which would be beneficial to

274   its solubility. γ-decalactone was found to blend at a 50:50 ratio without butanol in the diesel

275   fuel, however, to maintain consistency, the same blend ratios were used for all tests. The

276 enhanced solubility of γ-decalactone is due to the long side chain of the lactone, producing a

277 degree of non-polarity within the molecule that allows the formation of intermolecular forces

278 with diesel fuel molecules, which are typically made up of long aliphatic chains.

279

280 **Table 2.3: Lactone blending ratios**

Diesel Volume	Butanol Volume	Lactone Volume	Lactone Volume %
150ml	50ml	100ml	33

281

282 A 50vol% diesel:butanol blend was also tested in this study to assess the relative effects

283 of replacing butanol with the various lactone molecules.

284 A Brookfield digital rheometer was used to measure the viscosities of the blended fuels

285 (Figure S1-S2). This equipment operated using a spindle, immersed within the test fluid, driven

286 through a calibrated spring. The deflection of the spring provides details of the viscous drag

287 of the fluid which can be converted into viscosity (in centipoise) using the known rotational

288 speed, size/shape of the spindle and container, as well as the torque of the spring. The

289 specifications of the rheometer can be found in Table S1 (Supplementary Information). The

290 temperature was controlled with a water bath, maintained at 20 °C and circulated around and

291 through the jacket holding the test fluid. Important to note is that, before submerging the

292 spindle in the container of test fluid, the instrument is autozeroed. Once completed, the spindle

293 is submerged and the instrument reads a viscosity value. Monitoring of the viscosity over a

294 period of 5 minutes was important to ensure any drift (caused by shear thinning for example)

295 was observed as a result of the rotation of the spindle. No drift was observed for these tests,

296 therefore the viscosity value recorded after 5 minutes was deemed the final value.

297

298 ### 2.3. Research engine

299

300 A direct-injection, custom built, 4-stroke single cylinder compression-ignition engine was

301 employed in these experiments. The cylinder head, intake manifold, fuel injector, piston and

connecting rod were from a Ford Duratorq, 2L turbocharged engine (CD132 130PS). A Ricardo Hydra single cylinder crank case was employed. Further details of the engine and its auxiliaries can be found in previous work published by the group, while a schematic of the entire setup can be found in Figure S3 (Supplementary Information).[17] Measurements of in-cylinder pressure and exhaust gas composition were taken for all experiments.

Table 2.4: Diesel engine specifications

Engine Head Model	Ford Duratorq
Engine Crankcase Model	Ricardo Hydra
No. of Cylinders	1
Cylinder Bore (mm)	86
Cylinder Stroke (mm)	86
Swept Volume (cm^3)	499.56
Geometric Compression Ratio	18.3 : 1
Max In-Cylinder Pressure (bar)	150
Piston Bowl Design	Central ω bowl
Fuel Injection Pump	Delphi single-cam radial-piston pump
High-pressure Common Rail	Delphi solenoid controlled (Max 1600 bar)
Diesel Fuel Injector	6-hole solenoid valve injector (Delphi DFI 1.3)
Fuel Injection System	1 µs duration (EMTRONIX EC-GEN 500)
Crank Shaft Encoder	1800 ppr (0.2 CAD resolution)

2.4. High pressure, low volume (HPLV) fuel system

A low volume fuel system was employed for the injection of the novel fuels into the combustion chamber (Figure S4- Supplementary Information). This was due to a combination of the cost of some of these molecules, the physical properties, such as viscosity and density, which were not suitable to use in the standard common rail system, and the difficulty in cleaning the header tank and subsequent common rail fuel system from contaminants when testing different fuels consecutively.

This fuel system allowed tests to be conducted with low amounts of fuel (less than 1L). The system was easy to clean and reuse for different fuels, and avoided subjecting the fuel pump to potentially incompatible fuels. The stainless steel vessel encased a free moving piston which divides the vessel into two chambers; the one below the piston is connected to the

322 standard common rail injection system and therefore can be pressurised using the common

323 rail fuel system and diesel fuel. Mixing of the diesel and test fuel, as well as leaking of the

324 diesel or test fuel from either chamber, was prevented using Polymax Viton O-rings on the

325 lids, the top and bottom of the vessel and the piston itself.

326

327 **2.5. Engine Operation**

328

329 The engine was operated at a constant engine load of 4 bar IMEP and a constant engine

330 speed of 1200 rpm. The lactone blends were tested at only constant start of combustion timing,

331 with the start of injection varied according to the ignition delay of each fuel so that the start of

332 combustion always occurred at TDC.

333 A constant injection pressure of 550 bar was utilised for all tests, with the injection duration

334 and timing modified for each fuel to maintain a constant engine load of 4 bar IMEP and start

335 of combustion at TDC. A summary of these injection parameters is outlined in Table 2.5 below,

336 with diesel injection characteristics - at the start and end of a testing day- supplied to highlight

337 any major changes in injector performance across a day.

338

339 **Table 2.5: Injection parameters for the blends tested (4bar IMEP, 1200rpm)**

Fuel	Average Injection Duration (µs)	COV of Injection Duration (%)	Injection Timing (CAD BTDC)
Base Diesel (Start)	593	0.3	9.6
ε-caprolactone	658	0.99	14.5
δ-hexalactone	659	0.37	14.3
γ-caprolactone	648	0	14.2
γ-decalactone	637	0.11	12.6
Butanol	638	0.23	14.6
Base Diesel (End)	594	0	9.8

340

341 The pure lactone fuels were tested under the same engine load and speed conditions

342 as those of the lactone blends. For these pure fuels, both constant injection (CInj) and constant

343 ignition (CIgn) tests were undertaken. At constant injection timing, the start of injection was

344 kept constant at 10 CAD BTDC and the start of combustion allowed to vary in accordance with

345 the ignition delay of each fuel. This additional condition was employed due to the testing of

346 pure fuels were tested, with a greater range of ignition delays anticipated, and it was important

347 to discern whether differences in combustion characteristics were caused by combustion

348 phasing or the fuel chemistry. At constant ignition timings, the observed ignition (point at which

349 the apparent net heat release rate became positive) was controlled at 360 CAD by altering the

350 injection timing. A summary of the injection properties is supplied in Table 2.6 below. It was

351 noted that these values were consistent across all tests and fuels, likely due to the effective

352 lubrication of the injector by the high viscosity lactone fuels.

353 **Table 2.6: Injection durations and timings of pure lactone fuels and base diesel tests (4bar**

354 **IMEP, 1200rpm, SOI = 10 CAD BTDC for CInj tests)**

Fuel	CInj Average Injection Duration (µs)	CInj COV Injection Duration (%)	CIgn Average Injection Duration (µs)	CIgn COV Injection Duration (%)	CIgn Injection Timing (CAD BTDC)
Diesel	592.5	0.25	591	0.15	9.6
δ-decalactone	691	0.18	694.5	0.28	12.6
γ-dodecalactone	678.5	0.27	679.5	0.30	9
δ-dodecalactone	679	0.37	685.5	0.12	10
γ-decalactone	687	0.71	694	0.26	11.8

355

356

357

358

359

360

361

362

363

364

365

366

3. Results and discussion

3.1. Diesel-butanol-lactone blend results

3.1.1. Combustion Characteristics
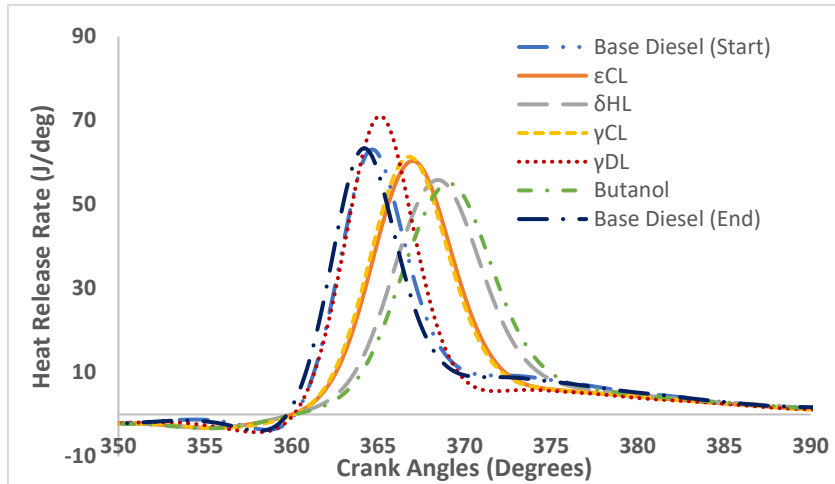

Figure 3.1: Apparent net heat release rates during combustion of diesel-butanol-lactone blends and base diesel at 4 bar IMEP, 1200 rpm and constant start of combustion at TDC

Figure 3.1 shows the apparent net heat release rates of the various diesel-butanol-lactone blends, compared to fossil diesel. The tests were conducted at constant ignition conditions, which ensured that heat release occurred at similar in-cylinder volumes. Heat release during diesel combustion at the start and end of a test day are shown to highlight the range of experimental variation. Apparent from Figure 3.1 is the subtle difference in the heat release rates of base diesel start and base diesel end, suggesting the variation in heat release between the lactone blends to be attributable to the fuel composition and not drift in engine performance. Of the fuels tested, the sharpest rise in heat release rate is seen in the case of base diesel start and base diesel end, followed by yDL and with the slowest increase in heat release rate apparent during combustion of the δHL and the butanol-only blend. Interesting to note is that the yDL blend exhibited a higher peak heat release rate than base diesel, likely owing to the longer ignition delay of the former that allows more time to form a homogenous fuel-air mixture (observable from the start of injection, indicated by the negative HRR slope in

16

395 Figure 3.1, occurring just after 350 CAD). γCL and εCL produced peak heat release rates of

396 comparable magnitude, occurring slightly later compared to those exhibited by the base diesel

397 and the γDL blend. More rapid combustion is expected in the case of γCL, given that the ethyl

398 chain will likely help produce the radicals necessary to fully open the lactone ring and enhance

399 flame propagation. However, it is unclear why similar combustion phasing was exhibited by

400 εCL given the absence of an alkyl chain to provide readily available sites for hydrogen

401 abstraction.

402 Relative to δHL (with one methyl branch), the lack of any side chains in εCL might be

403 expected to reduce ignition quality and combustion stability. Figure 3.1 indicates that this is

404 not the case, with δHL exhibiting a lower magnitude and later timing of pHRR, suggesting that

405 the structure of δHL reduces rates of combustion. Since both injection and ignition timings

406 were similar for both molecules, it is likely that initial radical formation is not the pathway that

407 is hindered, and instead δHL derivatives may result in more chain terminating reactions. δHL

408 combustion appeared similar to that of the diesel:butanol 'control' blend, with both blends

409 resulting in relatively unstable combustion. Butanol has been commonly employed in diesel

410 testing[40]- under a range of conditions- but blend ratios greater than 20 vol% have been shown

411 to result in poor combustion efficiency and high CO emissions.[43]
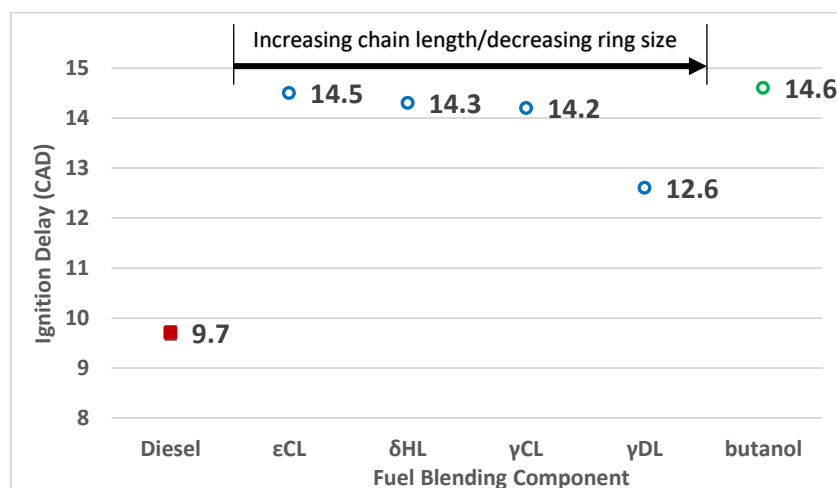
412

413 **Figure 3.2: Duration of ignition delay of the lactone and butanol blends, and base diesel, at**

414 **constant engine speed and IMEP and variable injection timing for constant start of combustion**

415

Figure 3.2 shows the duration of the ignition delay period during combustion of the lactone and butanol blends and also the base diesel. Immediately apparent in Figure 3.2 is the consistent repeatability in measurement of ignition delay as signified by the minor error bars on the base diesel data point, calculated from the standard deviation of all base diesel repeats. The lactone/butanol blends all exhibited longer delay periods than the base diesel. Given the fact that the longest delay period was exhibited by the butanol blend, it is apparent that all the lactones tested possessed higher ignition quality as a blending component than the short chain alcohol. This is expected, given the low cetane number (15.92) of butanol[44] and the higher carbon number of the lactones compared to the four carbons in butanol. With a variation of only 20% of the blend content, it can be seen that the duration of ignition delay is not changed significantly between the three C6 lactones (ε-caprolactone, δ-hexalactone, γ-caprolactone), with the longest ignition delay exhibited by εCL and the shortest by γCL, indicating a trend of decreasing ring size and longer side chain length reducing the duration of the delay period. With a further increase in the length of the side chain at constant ring size (γ-decalactone relative to γ-caprolactone) the delay period is reduced more substantially, (12.6 CAD from 14.2 CAD). Recalling again that only 20% of the blend content is varied between the lactone blends, and yet the delay period decreases by over 1 CAD, suggests that γ-decalactone is a highly ignitable fuel compared to the other lactones tested in these blends. While a higher fuel viscosity may be expected to be detrimental to fuel atomisation, therefore decrease ignition propensity, the long-side chain of γDL generates the necessary chemical reactivity to counteract this effect and readily ignite in a compression ignition engine.

3.1.2. Gaseous emissions
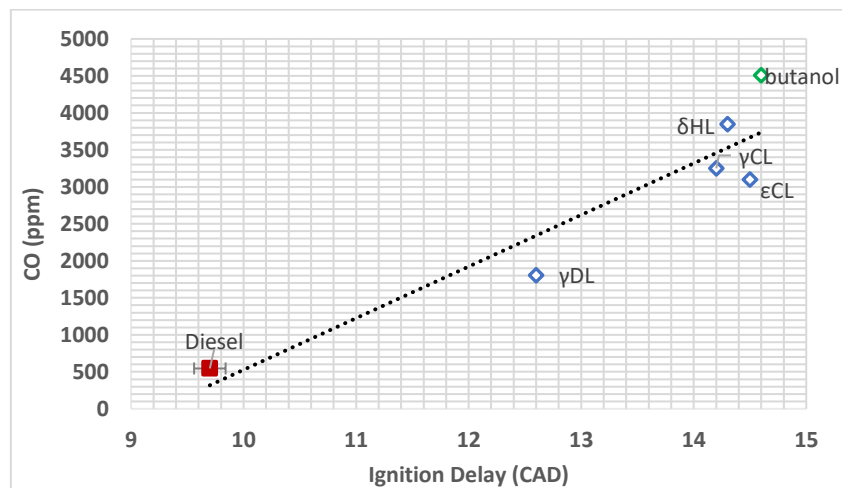

***Figure 3.**3: Exhaust gas concentrations of CO and duration of ignition delay during combustion of the lactone blends and base diesel*

The combustion efficiency can help illustrate, to a large degree, the compatibility of a given fuel with a compression ignition engine. Figure 3.3 shows the measured exhaust gas concentrations of CO of the lactone blends relative to the duration of ignition delay and indicates the extent of incomplete combustion, where higher emissions of CO imply more incomplete combustion. Figure 3.3 indicates a positive trend of CO emissions with increasing ignition delay. With increasing duration of ignition delay it is likely that the fuel becomes increasingly overdiluted with air, with areas of the combustion chamber becoming too fuel lean for combustion to occur. The excessively ignition delay of the blends can largely be attributed to the butanol within the blend (the diesel:butanol blend possesses the highest CO emissions), although the 6-carbon lactones also contribute to this given their relatively low carbon number and high oxygen content, and therefore low ignition propensity (Figure 3.2). This extended delay period not only causes over dilution, and therefore lower combustion temperatures- reducing reaction rates and therefore the proportion of complete combustion- but also increases the likelihood of fuel impingement on the cylinder walls.

The higher density of these lactones (see Table 2.1) compared to diesel (with a density of approximately 0.85g/cm^3) is a property that has been shown to increase lift-off length of fuel sprays, thus increasing the likelihood of droplets reaching the walls.[45] The lactones also

465 possess higher viscosities than diesel itself (diesel viscosity: ~ 1.35 mPa s)[46], making fuel

466 atomisation poorer and resulting in a greater proportion of fuel-rich, oxygen deficient zones

467 where CO may form. A further physical property to consider though is the boiling point; ε-

468 caprolactone and δ-hexalactone are relatively volatile, with boiling points of 98°C and 111°C

469 respectively. It is therefore postulated that, for these lactones and butanol in particular, fuel

470 penetration into the chamber is relatively low, with a vapour cloud close to the injector tip

471 potentially forming, which could be responsible for incomplete combustion due to a lack of

472 oxygen entrainment.[47,48]

473 γ-caprolactone possesses a boiling point of 219°C, far higher than the other two C6

474 lactones. However, this blend produced levels of CO similar to those during combustion of ε-

475 caprolactone, therefore physical properties do not entirely explain the trends in CO emissions,

476 though ignition delay is a clear contributor. δ-hexalactone sees the highest CO emissions and

477 therefore degree of incomplete combustion. Since the delay period decreases from the largest

478 to smallest ring, the ID does not fully explain the difference in CO emissions, which increase

479 from seven to five to six-membered rings, though these differences are relatively minor (Figure

480 3.3). A tentative suggestion, however, is that, because δ-hexalactone possesses the highest

481 density, this fuel spray possesses the greatest momentum during injection and is most likely

482 to become impinged onto the cylinder walls when coupled with the long ignition delay periods

483 observed in these C6 lactone and butanol blends.

484

485

486
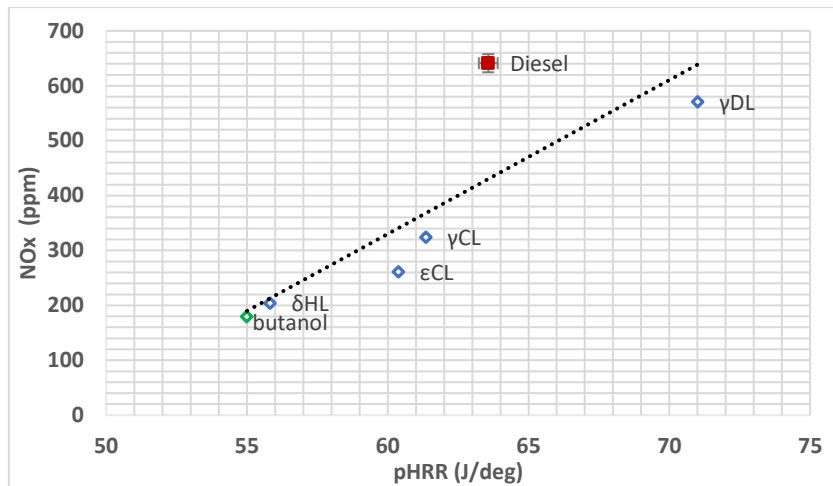
Figure 3.4: NOx emissions and peak apparent heat release rate lactone butanol diesel blends
at constant ignition timing

489

490   Figure 3.4 shows the exhaust levels of NO_x relative to the peak apparent net heat release
491   rates during combustion of the lactone-butanol-diesel blends and base diesel at constant
492   IMEP and start of combustion at TDC. Apparent is the significantly lower NO_x concentrations
493   emitted by the lactone blends compared to the base diesel, which consistently produced
494   approximately 640 ppm; the error bars show plus and minus one standard deviation from the
495   mean and indicate the high degree of repeatability in NO_x measurement during diesel
496   combustion. The lowest NO_x levels were observed for the butanol blend and can likely be
497   attributed to the more unstable combustion in the case of this blend- noted by the high CO
498   emissions (Figure 3.3)- and thus could be expected to yield lower in-cylinder temperatures on
499   average. Given the fact that NO_x emissions are formed from the oxidation of nitrogen- and
500   therefore rates of formation increase with increasing temperature- this decrease in
501   temperature corresponds to lower NO_x.

502
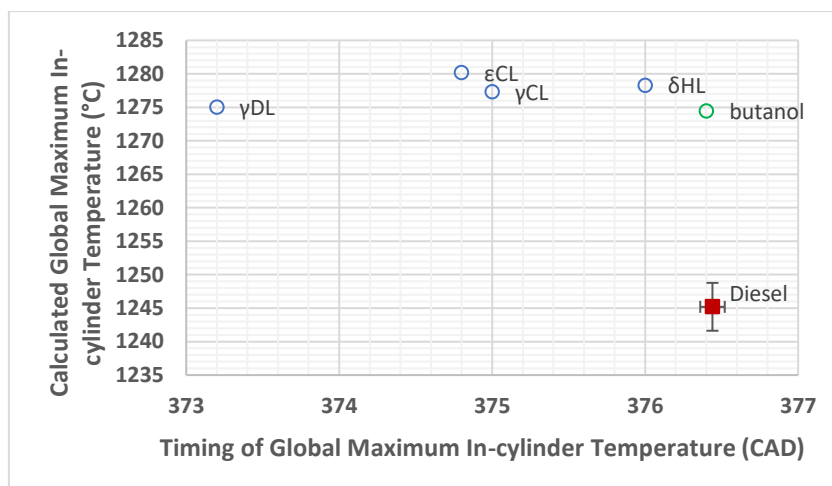
Figure 3.5: Magnitude and timing of calculated maximum global in-cylinder temperature of blended lactone-butanol-diesel fuels and base diesel

Figure 3.5 shows the calculated maximum global in-cylinder temperature and time of occurrence for the lactone blends and base diesel. Contrary to the lower temperatures suggested by the NO_x emissions (Figure 3.4), Figure 3.5 indicates that the butanol blend exhibited comparable maximum in-cylinder temperatures when compared to the lactone blends, and at a timing equivalent to that of base diesel. Also illustrated are the considerably lower maximum in-cylinder temperatures experienced during diesel combustion compared to the lactone blends. However, the timing of the peak HRR and maximum global temperatures, shown in Figure 3.6 below, offers potential reasoning for higher NO_x during diesel combustion as compared to the lactone blends. Figure 3.6 shows that the duration between peak heat release rate and maximum in-cylinder global temperature is approximately 12 CAD. Comparing this to butanol blend combustion, where the difference is closer to 7 CAD, suggests more sustained combustion in the case of diesel and therefore the temperatures necessary for NO_x formation are likely prolonged.
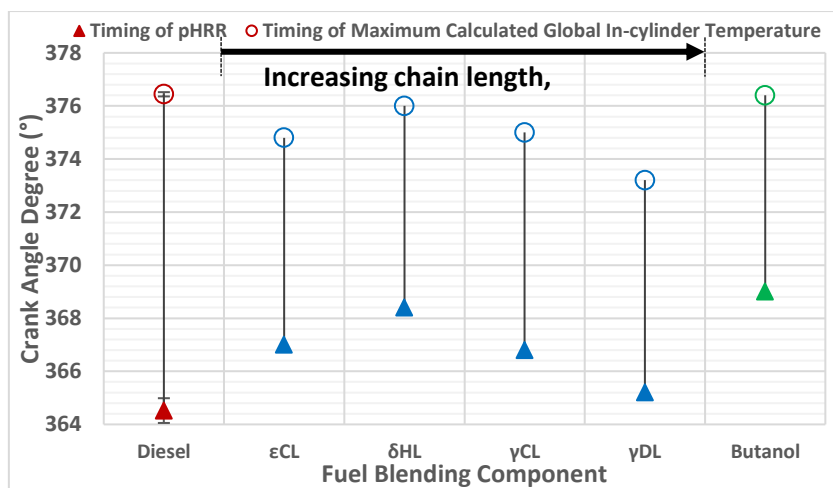
Figure 3.6: Time of occurrence of peak HRR and peak calculated global in-cylinder temperature of fuel blends and base diesel

Higher pHRR and sufficient duration of sustained high combustion temperatures, occurring close to TDC, also helps to explain why the blend of γ-decalactone produced the highest NO_x emissions of any of the lactone blends tested, despite having the shortest ignition delay period that often results in lower NO_x emissions due to a reduction in premixed combustion. The strong ignition properties of γDL enabled pHRR to occur earlier in the expansion stroke (compared to other test blends), shown in Figure 3.1 and 3.6, where higher cylinder pressure conditions were attained. Thus, high temperatures could be maintained with the reduced cylinder volume reducing rates of heat transfer to the exposed wall surface area. Furthermore, the presence of two oxygen atoms within the γDL molecule will potentially have resulted in higher adiabatic flame temperatures, compared to fossil diesel (containing no oxygen). While the advanced combustion phasing in the case of yDL (Figure 3.2) is beneficial to combustion efficiency, resulting in a reduction in incomplete combustion products such as CO (as noted in Figure 3.3), the higher temperatures result in higher NO_x (Figure 3.4).

Considering the C6 lactones, the longest delay period and highest maximum in-cylinder temperatures are observed with ε-caprolactone, though γ-caprolactone produced higher NO_x emissions. A shorter delay period generally reduces fuel-air premixing and therefore the potential magnitude of pHRR (thereby reducing energy release and temperature). However,

as shown in Figure 3.4, for the C6 lactones, the NO_x emissions are in agreement with pHRR, while the period between pHRR and peak temperature (Figure 3.6) is marginally longer in the case of γ-caprolactone. The increase in NO_x emissions seen in the case of γ-caprolactone may also be explained by an improvement in combustion quality as a result of the ethyl chain on this lactone, as indicated by the shorter duration of ignition delay (Figure 3.2). The ethyl chain, and the radicals that may be produced from this, may have helped to sustain higher combustion temperatures, offsetting the effect of butanol within the blends; the butanol diesel blend emitted the lowest NO_x levels (Figure 3.4), attributable to its poor combustion properties (Figure 3.1 and 3.2) and delayed time of peak heat release rate (Figure 3.6).

It consistently appeared that δ-hexalactone possessed significantly unfavourable combustion characteristics compared to the other C6 lactones, with pHRR and peak in-cylinder temperature occurring later (Figure 3.6), despite a comparable ignition delay (Figure 3.2) to that of εCL, and higher CO emissions produced (Figure 3.3). The lower NO_x emissions produced with this blend continue to suggest poor combustion efficiency. Injection timings were similar for all C6 lactones as a result of the similar ignition delay period, and the start of combustion commenced at 360 CAD in all cases. The physical properties shown in Table 2.1 do not appear to reflect major discrepancies in volatility and density, but important to note is that the blending of δ-hexalactone was the poorest of all lactones, despite it seemingly representing a mid-point between ε-caprolactone (no side chain) and γ-caprolactone (ethyl chain), suggesting that competing molecular characteristics are at play. One hypothesis is that the structure of δ-hexalactone, and or its subsequent decomposition products, is not conducive to combustion, potentially inhibiting initiation or propagation reactions. Six-membered ring structures are the most stable cyclic molecules,[49] and therefore, while the methyl group may allow for some release of radicals, it could be that this ring structure is the most difficult to open of the lactones tested, and the reactants produced from the methyl chain are not sufficient in breaking this ring early in the premixed combustion phase.
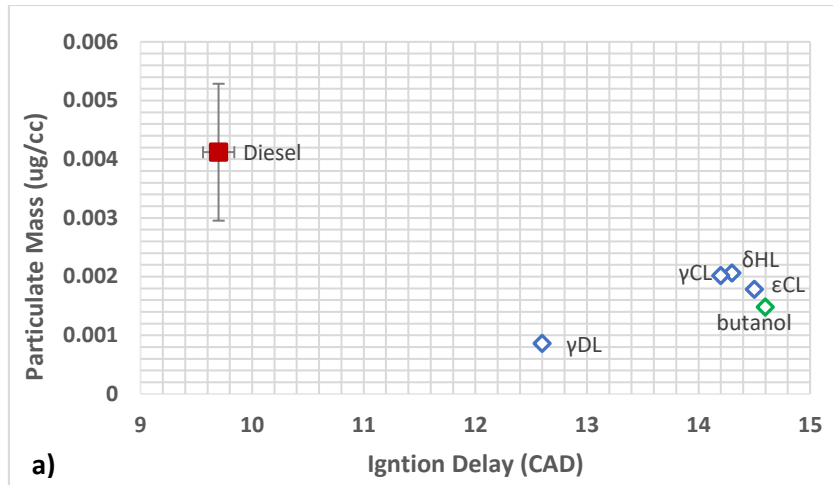
3.1.3. Particulate emissions
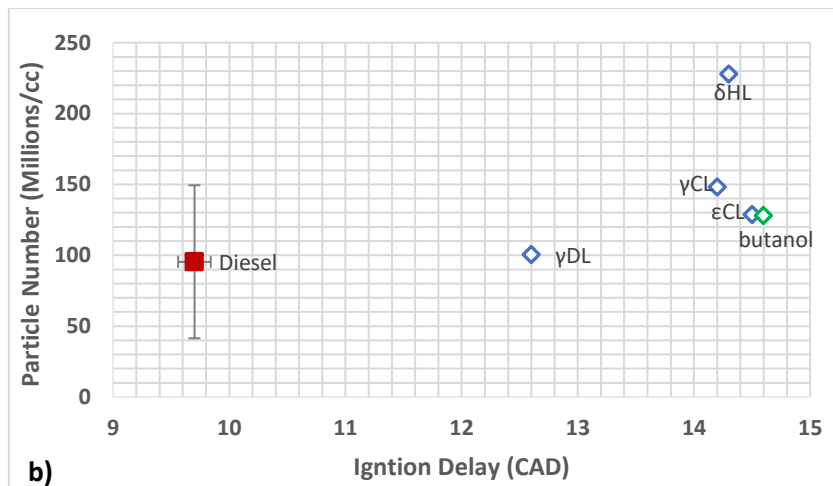
Figure 3.7: Trend between particle mass (a) and particle number (b) with ignition delay of lactone and butanol blends and base diesel (start and end)

Figure 3.7 indicates that particulate emissions were more variant than other emissions tested, reflected in the error bars in Figure 3.7, which encompass a significant range of results that includes the majority of the results of the blended fuels. A potential explanation for this is an increase in engine efficiency from the start to the end of a test day, with higher oil temperatures and a faster acting injector employed as testing ensued, following warm-up and lubrication by the test fuels. Therefore, the following conclusions are stressed as suggestive. Notwithstanding the range of error presented, it can be seen from Figure 3.7 that all of the lactone-butanol-blends emitted a significantly lower level of particulate mass relative to diesel

584   only combustion, which is in line with the extended ignition delay that could allow for greater

585   fuel-air mixing and a reduction in fuel-rich zones in which particulate formation is prevalent.

586   The particulate mass and number output from the combustion of 'biofuels' often contrasts

587   significantly with the emissions from purely fossil diesel combustion;[50] the particulate mass

588   generally decreases substantially, while the particle number increases as a result of the

589   formation of more, smaller particles in the case of the blends.[51,52] A significant contributor to

590   the reduction in particle mass (other than the aforementioned extended ID) is likely the oxygen

591   present in the lactones, which seemingly increased rates of oxidation of particulates post-

592   formation, rendering particulates exhausted smaller. It is also likely that the phasing of soot

593   formation is shifted slightly with the longer ignition delay period seen in these bio-derived

594   molecules, not only decreasing particle mass but increasing number. The formation of

595   particulates occurs later in the blends, therefore there is less time (and also a greater in-

596   cylinder volume) in which the particles are able to form and grow.
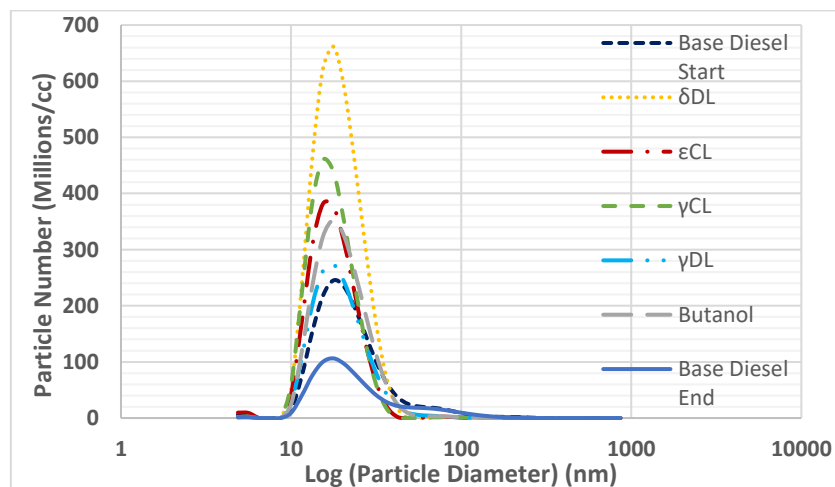
597

598   *Figure 3.8: Particle size distribution of lactone and butanol blends and base diesel (start and*

599   *end)*

600   The reduced soot agglomeration and coagulation afforded by the retardation of

601   combustion in the case of the lactone blends can be seen from the particle size distribution

602   plot in Figure 3.8. Also apparent is the significant increase in small particles of δHL in

603   particular. Comparing the C6 lactones tested to the butanol:diesel blend, an increase in

604   particle mass and number (although the particle number output of butanol and ε-caprolactone

605   were very similar) was noted in the case of the lactones (despite an increase in oxygen

606   content) which is counter to the view that the poor combustion quality of butanol (Figure 3.1)

607   may lead to the formation of more incomplete combustion products (Figure 3.3). This may be

608   due to the combustion of the butanol diesel blend being too unstable, with an excessive

609   ignition delay, to the extent to which particulates are not formed in great amounts since local

610   temperatures were not sufficient to produce pyrolysis products. Another potential explanation

611   is that the structure of the lactones is more inclined to result in greater particulate formation,

612   the higher carbon number providing greater availability of reactants for soot precursors.

613   Alcohols are one of the most effective oxygenated fuels in reducing particle formation, most

614   likely due to the single carbon-oxygen bond that renders the oxygen more available to oxidise

615   soot particles and reduce the particle mass.[53,54] The particle mass of all C6 lactones was

616   similar, the main difference in particle emissions is in the case of δ-hexalactone which

617   produced the highest particle number. As with CO emissions (Figure 3.3), it is not clear why

618   δHL has the greatest tendency to form incomplete combustion products compared to the other

619   lactones, and the aforementioned stability of this 6-membered ring structure and the

620   subsequent late release of energy could be the reason. Another theory put forward is that the

621   chemical structure of this 6-membered ring lactone is slightly more likely to produce soot

622   precursors. Until recently, soot particles were thought to consist predominantly of six-

623   membered ring species (benzenoids),[55] but studies have realised the potential of five-

624   membered rings (pentagonal) to be major factors in the morphology of soot particle, especially

625   introducing 'curvature' into the carbon nanostructures and becoming prevalent in incipient soot

626   particles.[56,57] Given that the structure of δHL is that of five carbons within the cyclic ester

627   moiety, and the addition of a methyl chain, it is tentatively suggested that the breakdown of

628   this molecule has a higher tendency to form these five-membered rings that are effective in

629   amalgamating PAHs. It is not unreasonable to expect that the carbons within the ring of δHL

630   do not always separate if the ring structure is not broken until significantly into the expansion

631   stroke. More certain is the shift in combustion with δHL (and butanol), which results in pHRR

occurring later in the expansion stroke (Figure 3.1 and 3.6). Therefore, a likely cause of the higher particle number for a given mass is that the particles have less potential to agglomerate at these higher volume conditions, closer to the exhaust stroke. The difference between δHL and butanol in terms of particle number, however, is the strong oxidative capability of the alcohol, which reduces overall particle mass and number.

The reduced particle mass and slightly reduced particle number produced by γ-decalactone, compared to the other lactone blends, is a surprise given the significant increase in carbon number of this lactone. Likely, this can be at least partially attributed to the higher combustion temperatures (Figure 3.5) that enhance the rate of soot oxidation, reducing particle mass. Furthermore, the boiling point of γDL is significantly higher than in the other blends, potentially increasing lift-off length, which tends to see a reduction in particulate emissions as this increases the available oxygen entrained, thereby lowering the premixed equivalence ratio.[58] Moreover, when a tertiary fuel blend is combusted, and possesses vastly different boiling points, it can undergo a micro-explosion phenomena.[43] The more volatile component- butanol in this case- will vaporise within the bulk droplet and essentially 'explode', fractionating the main fuel droplet more effectively and reducing pyrolysis regions.

3.2. Pure lactone fuels

From the lactone blend study, it was apparent that a long alkyl chain attached to the ring of a lactone was effective in reducing the ignition delay period, the CO emissions, and both particle mass and number. Furthermore, the ability to blend the high carbon number molecules- with non-polar side chains- in higher ratios than the C6 lactones, and without butanol, is advantageous from both a combustion perspective (butanol is a poor compression ignition fuel) and reducing reliance on fossil fuels. A 50:50 blending ratio would be achievable, however tests were subsequently conducted to assess the viability of the C10-C12 lactone fuels (Table 2.2) as pure components without the presence of any fossil diesel fuel. Not only

659   would this enable the combustion performance of the individual fuels to be determined more

660   accurately, but successful combustion would indicate that conventional diesel molecules need

661   not be used in compression ignition engines in the future.

662

663   3.2.1. **Combustion characteristics**

664   Both constant injection and constant ignition tests were possible in the experiments with

665   pure lactones, due to the stable combustion traits that all test fuels displayed. At constant

666   injection (CInj) conditions, all fuels experienced equivalent physical conditions during the

667   ignition delay period while, for constant ignition (CIgn) combustion, all fuels were exposed to

668   the same conditions at the start of combustion.
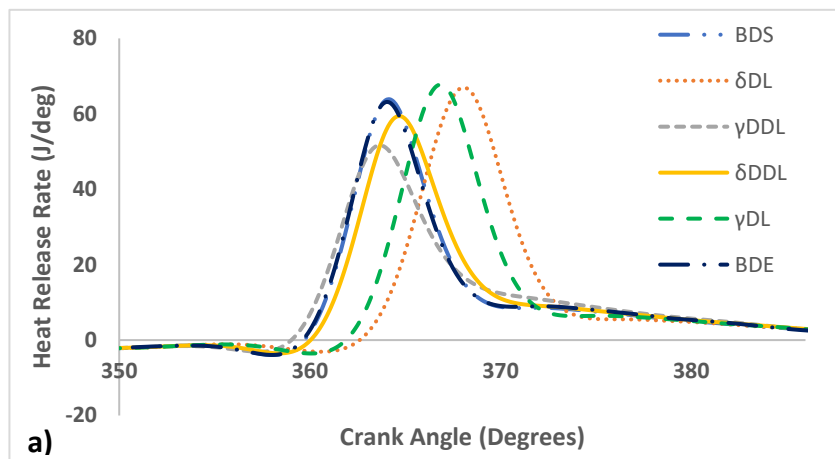
669

670
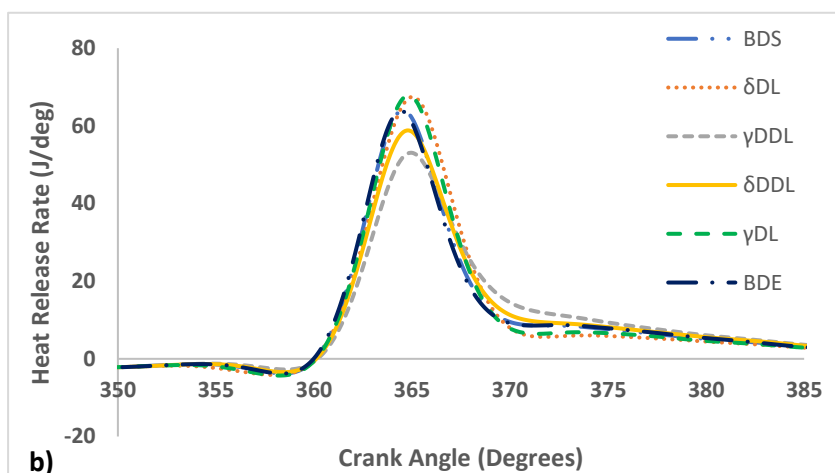671
672
673
674
675

a)

676

677
678
679
680
681
682

683

b)

684

Figure 3.9: Apparent net heat release rates during combustion of lactone fuels and diesel fuel (start and end) at constant injection (a) and constant ignition (b) conditions at 4 bar IMEP, 1200 rpm and constant start of combustion at TDC

From Figure 3.9, comparing base diesel start and base diesel end it is apparent that the engine drift in terms of heat release during the pure lactone tests was negligible. Figure 3.9a also shows that three out of the four pure lactones tested exhibited longer ignition delays than the base diesel (indicated by line intersections of the x-axis occurring further to the right than the base diesel lines), with the exception being γ-dodecalactone (γDDL). The reduced premixing time of this C12 lactone can be seen to reduce pHRR compared to diesel. Its isomer, δ-dodecalactone, displayed a slightly longer delay time than diesel, though produced a slightly decreased pHRR, indicating that mixing was less efficient for this fuel. Table 2.2 shows the boiling points of the lactone fuels. The low volatility, of the C12 lactones in particular, was potentially detrimental to fuel vaporisation,[45] resulting in reduced premixing of fuel and air and therefore lower pHRR, and more of the fuel being burnt in the diffusion-led combustion phase relative to diesel. The two C10 lactones, as pure fuels, resulted in marginally longer delay periods than diesel, and thus resulted in higher pHRR. The aforementioned low volatility of δ-dodecalactone was not as pertinent in these C10 molecules of lower atom number (Table 2.2).

Comparing constant injection and constant ignition experiments, it can be seen that the γ-dodeclactone test registered a pHRR earlier than that of diesel when injection was constant, but marginally later when ignition timing was maintained; in both cases the magnitude was lower. With constant injection timing, the shorter delay period of this lactone naturally resulted in an earlier pHRR, as combustion had been advanced slightly. During constant ignition tests however, the lactone injection was retarded slightly to compensate for the rapid ignition, thus delaying pHRR relative to diesel (diesel injection timing was similar for both CInj and CIgn tests).

A similar analysis can be made when comparing δDL to γDL. The former possesses a longer delay period- 0.6-0.7 CAD longer- and so when injection timings were changed to normalise ignition timing, the phasing of δDL and γDL combustion converge, indicating little change in the actual combustion rates of the 2 lactones once ignition reactions have initiated. However, δDL has more time to mix with air, so the fact that the pHRR does not increase suggests there is more unreacted fuel, or incomplete combustion, from this fuel compared to γDL.
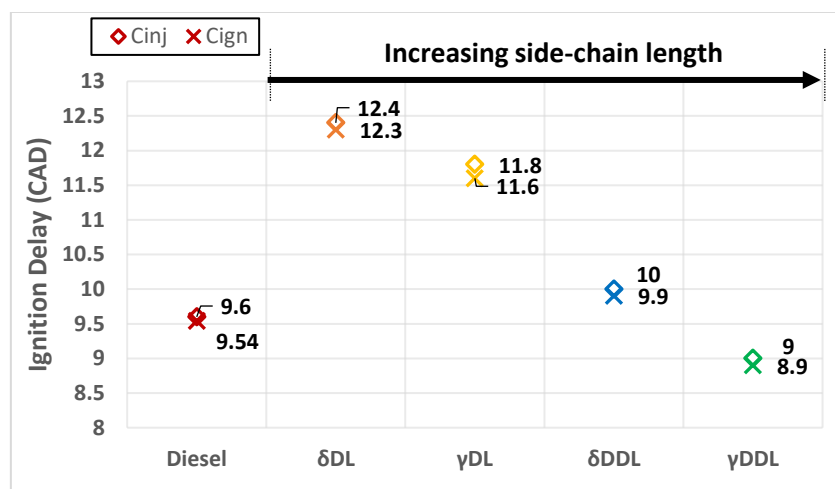
Figure 3.10: Duration of ignition delay of lactone fuels and base diesel (diesel results are calculated averages) at constant engine speed and IMEP and variable injection timing for constant start of combustion

The durations of ignition delay shown in Figure 3.10 enable some conclusions to be drawn from the use of a pure lactone fuel in a compression ignition engine. First of all, it is apparent that these lactones, despite possessing oxygen that tends to increase the delay period of a fuel molecule,[54,59] exhibit encouraging ignition properties relative to diesel. Figure 3.9 indicates that none of the pure lactones tested possessed delay periods long enough for combustion to become unstable. The shortest delay period was noted in the test of γ-dodecalactone, possessing a delay period of 9 CAD at constant injection timing, which was even lower than that of fossil diesel (Figure 3.10). It can be seen that the gamma-lactones have shorter ignition delays than the delta analogues, with γ-dodecalactone possessing a delay period of

approximately 9 CAD, while δ-dodecalactone exhibiting a longer delay period of 10 CAD. Naturally, the 10 carbon lactones are slightly less susceptible to ignition with a shorter chain lengths and overall atom number, but a delay period of between 11.8 and 12.4 for γ-decalactone and δ-decalactone respectively is still promising, considering no fossil diesel was used. These results indicate the importance of the increasing chain length of the side chain in increasing ignition propensity and, likely, the resulting combustion quality; these appear to be of greater influence on the delay period than the size of the ring, which likely breaks apart at a later phase after which enough radicals have been formed from the side chain for ignition to ensue.

3.2.2. Gaseous emissions
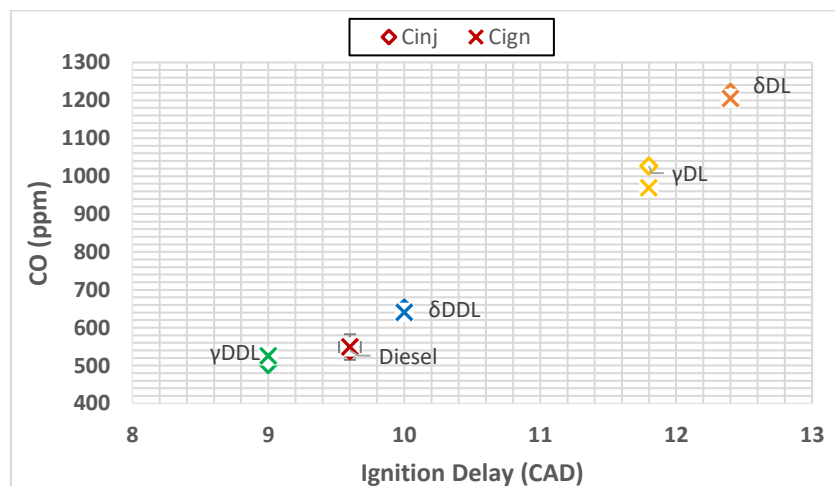
Figure 3.11: Relationship between carbon monoxide emissions and ignition delay of pure fuels at constant injection and constant ignition conditions

Figure 3.11 indicates that, for the pure lactones, CO emissions follow a trend of increasing with increasing ignition delay, in agreement with the lactone blend combustion results (Figure 3.3). The same reasons are put forward in explanation; a greatly extended ignition delay potentially leads to combustion at lower temperatures from over dilution and heat release during the expansion stroke; also, an increased viscosity fuel (Table 2.2 indicates the high viscosity of the lactones tested as pure fuels) leads to poor atomisation, thus larger fuel

753 droplets, impeding fuel-air mixing which can result in incomplete combustion through a lack of

754 oxygen available. Poor fuel vaporisation also increases the chance of droplets reaching the

755 cylinder wall and becoming impinged on the cold surface, where complete combustion is

756 unlikely.

757   At both constant injection and constant ignition timings, δ-decalactone emitted the highest

758 levels of CO and exhibited the longest duration of ignition delay (Figure 3.11). γ-

759 dodecalactone, with a delay period even shorter than that of diesel, displayed slightly lower

760 CO emissions than the fossil fuel, implying that the reduced premixing time available in the

761 case of the lactone did not result in excessive fuel-rich zones favouring CO formation. The

762 inclusion of oxygen in a molecule has been shown as advantageous in reducing CO

763 emissions[12] relative to diesel, with the occurrence of oxygen deficient zones reduced.

764   It can be seen in Figure 3.11 that the tests at constant injection and ignition timing yielded

765 very similar results CO emissions for each fuel. For the fuels possessing longer delay periods

766 than diesel, the constant injection tests produced slightly higher levels of CO, as combustion

767 was retarded slightly (ignition began *after* 360 CAD), and potentially a reduced proportion of

768 complete combustion occurred. In the case of γ-dodecalactone, constant ignition tests meant

769 an injection timing slightly delayed compared to constant injection timing.

770
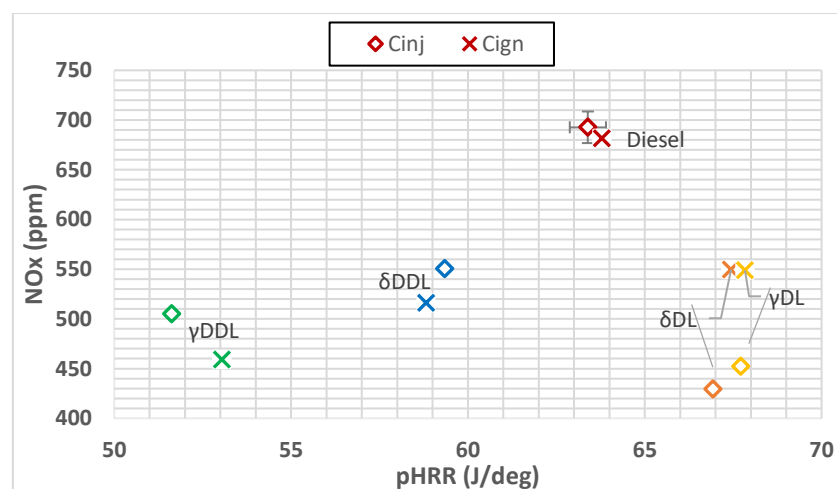
Figure 3.12: Exhaust gas nitrous oxide emissions and peak heat release rates for pure lactones and base diesel at constant injection and constant ignition conditions

774
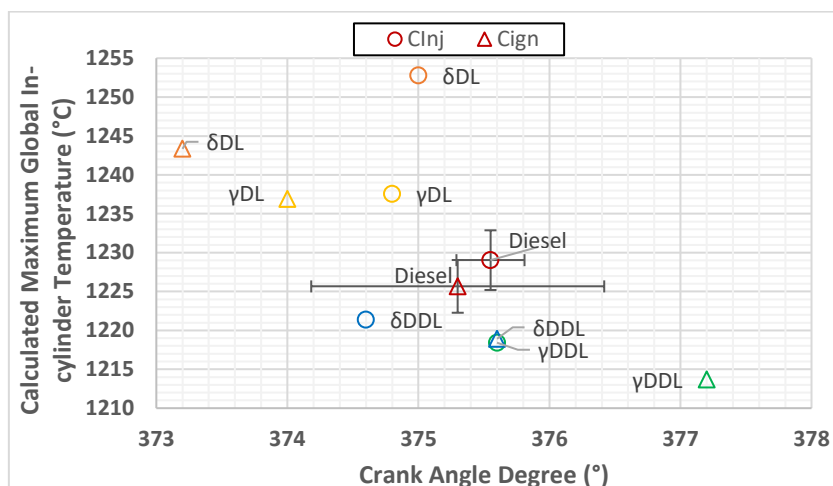
Figure 3.13: Magnitude and timing of calculated maximum global in-cylinder temperature of

pure fuels and base diesel at constant injection and constant ignition conditions

778

Clear from Figure 3.12 is that the emissions of NO_x from the diesel tests are consistently higher than that of the lactones, despite the pHRR of lactone combustion being comparable, if not higher, than diesel (Figure 3.9); as discussed in the context of the lactone-butanol diesel blends (Figure 3.4) NO_x emissions tend to relate to the magnitude of pHRR and resulting temperature. Figure 3.13 illustrates that the maximum magnitude of in-cylinder temperatures for diesel lay in the middle of those determined for the lactones, though the error bars suggest a significant degree of uncertainty. Therefore, instead of looking at only the magnitude of in-cylinder temperatures, it may be more informative to look at the timing of pHRR and peak temperatures (Figure 3.14).

Figure 3.14 shows that for constant injection testing, the timing of pHRR is earliest in the case of diesel and γ-dodecalactone, which could explain why diesel produces the highest concentration of NO_x (Figure 3.12); potentially, temperatures sufficient for NO_x formation were sustained for longer before exhausting the cylinder contents, alluded to in Figure 3.14 by the long duration between pHRR and peak in-cylinder temperature. γ-dodecalactone did not emit as much NO_x as diesel combustion however, despite the timing of the lactone pHRR being earlier than that of diesel in the constant injection tests, resulting in an even longer duration

795   between pHRR and peak global temperature. This can be attributed to the lower magnitude

796   of pHRR and peak temperature as a result of the shorter ignition delay period in the case of

797   γ-dodecalactone (Figure 3.9).

798   The two C10 lactones went against the trend of increasing NO_x with pHRR (and maximum

799   in-cylinder temperature). The combustion phasing again helps to explain this, with the shortest

800   duration between pHRR and peak temperature seen during combustion of these two fuels

801   (Figure 3.14). The CO emissions of the C10 lactones were also the highest of all fuels tested

802   (Figure 3.11), suggesting a reduced combustion efficiency. From the HRR shown in Figure

803   3.9, it can be seen that almost all of the heat release during combustion of the C10 lactones

804   occurs in the premixed phase, and it is possible that there are insufficient quantities of fuel left

805   in diffusion-led combustion to sustain the high temperatures necessary for NO_x formation.

806

807

808

809

810

811

812

813

814

815

816

817
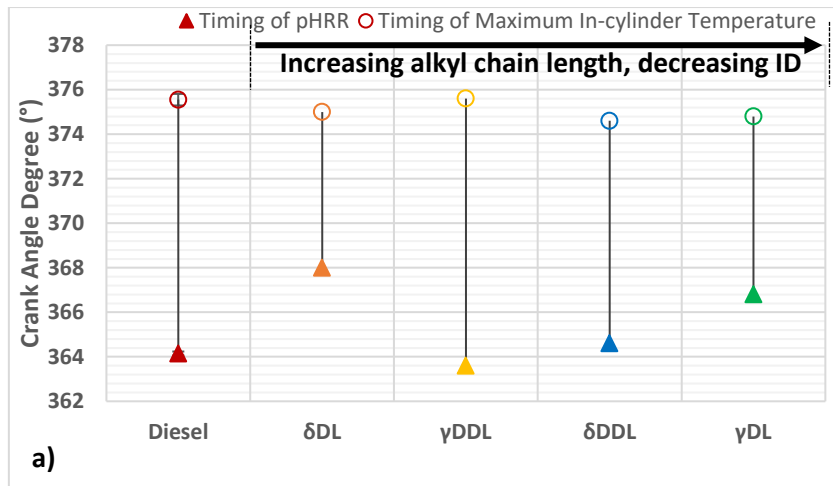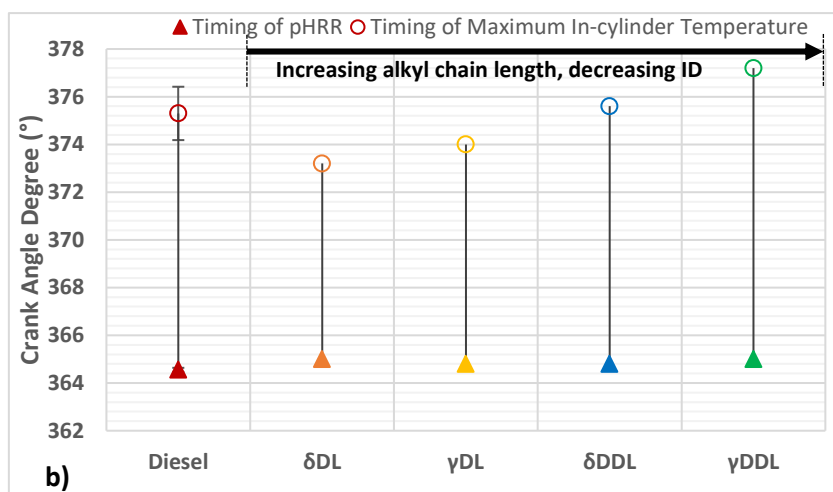
Figure 3.14: Comparison of timings of pHRR and peak in-cylinder temperature of pure fuels at constant injection (a) and constant ignition conditions (b)

820

A final note to make is the contrast in NO_x emissions when comparing constant injection and constant ignition tests. Whether the CInj or CIgn NO_x emissions were higher depends on the ignition delay of the respective fuels. Since the ignition delay of diesel was such that CInj and CIgn injection timings occurred at approximately the same time (Table 2.6; 9.6 CAD BTDC for CIgn, 10 CAD BTDC for CInj), there was little difference in NO_x emissions from diesel at these two timings. However, when the ignition delay was significantly lower than that of the reference diesel, as in γ-dodecalactone (Figure 3.10), constant ignition results resulted in lower NO_x emissions (Figure 3.12), which is likely because ignition was forced to occur later with the start of injection having been retarded. In the case of the tests at constant injection

timing, ignition occurred while the fuel-air mixture was still undergoing compression, and likely

this release of energy during the compression stroke saw significant NO_x formation due to

higher temperatures forming earlier and thus increasing time for the thermal NO_x formation

mechanism to occur. In the case of the C10 lactones, constant injection tests resulted in lower

NO_x exhaust concentrations (Figure 3.12). CInj tests saw ignition occur later than the CIgn

experiments, into the expansion stroke, where lower pressures meant that the majority of

energy was released at less favourable conditions for thermal NO_x to form. The fact that δ-

decalactone and γ-decalactone exhibited very similar levels of NO_x under constant ignition

conditions, suggests that the difference in NO_x emissions between the two fuels is almost

entirely due to the differences in the premixing phase.

3.2.3. Particulate emissions
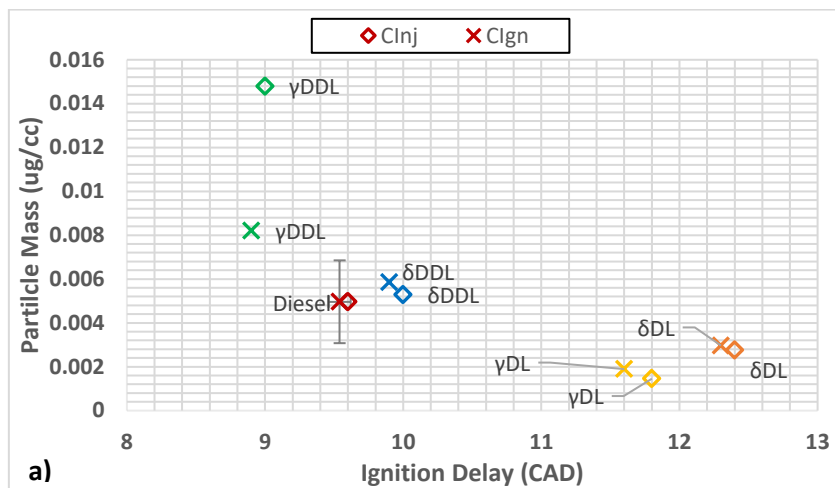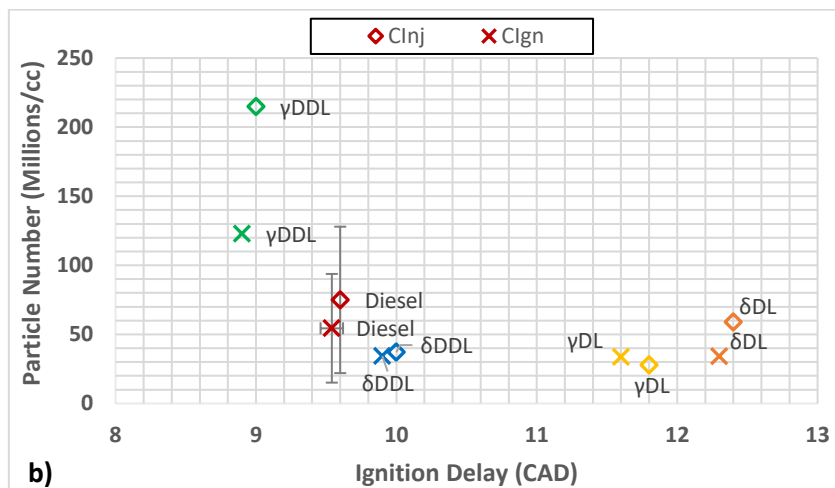
Figure 3.15: Relationship between particle mass (a) and particle number (b) and ignition delay of pure fuels at constant injection and constant ignition conditions

Important to note in Figure 3.15, firstly, is that measurement of particulates saw appreciable test to test variability, meaning conclusions as to the effect of the fuel itself are difficult to draw, noted by the major error bars.

Overall, both particle mass and particle number seemingly followed a general trend of decreasing ignition delay, likely caused by the reduced mixing durations increasing inhomogeneities in the fuel-air mixture. Compared to the combustion of the lactone butanol diesel blends, these pure lactone fuels behaved more comparably to neat diesel and did not possess significantly prolonged ignition delays (and therefore phasing), meaning that the

872   particle mass and number were more comparable. In lactone blends, however, the oxygenated

873   fuels saw a significant reduction in soot emissions on a mass basis, but an increase in the

874   particle number, suggesting smaller particles were present due to an increase in oxidation

875   and/or because particles were formed later and thus with insufficient time to form accumulation

876   mode particles.

877   Notwithstanding the error bars shown, Figure 3.15a shows that the emissions of particulate

878   mass are reduced in the case of γ-decalactone and δ-decalactone compared to diesel but

879   increased in the case of γ-dodecalactone. This was likely due to the short ignition delay of the

880   latter (Figure 3.10). The longer ignition delay of the C10 lactones (Figure 3.11) is also likely

881   responsible for the lower particle mass emitted relative to diesel, however the higher

882   oxygen:carbon ratio compared to the C12 lactones and diesel potentially decreases particle

883   mass also. Meanwhile particle numbers of the C10 lactones and diesel were comparable (and

884   the error bars in Figure 3.13b suggest assessments of these relatively small differences in PN

885   cannot be made).

886   Other than the reduced ignition delay resulting in less time for premixing of the fuel-air

887   mixture, it is suggested that a potential reason for the observed higher particle mass of the

888   C12 lactones (Figure 3.15a) is the length of the side chains present. It is not established how

889   the lactones studied break down during combustion, but the particulate mass in this instance

890   is in keeping with the number of carbons on the side chain of the molecule, increasing from γ-

891   decalactone (six carbons on the side chain) to δ-dodecalactone (seven carbons) to γ-

892   dodecalactone (eight carbons). Diesel fuel consists of numerous species, including long

893   chained alkanes, therefore it is not surprising that the PM emissions of the lactones and diesel

894   fuels are comparable, especially if one of the first stages of the molecular break-down of a

895   lactone involves separation of the side chain from the ring, or a ring opening reaction, which

896   would provide ample potential for soot precursors to form from radical attack on the resultant

897   long-chained alkyl chains. Pyrolysis products have been shown to increase as the chain length

898   of a molecule increases- even when keeping overall carbon numbers constant, likely as a

899   result of the weaker bond dissociation bonds of a longer molecule.[60]

Constant injection and ignition tests of the same fuels saw considerable variation of particle mass and number in some cases (Figure 3.15a and 3.15b). Notwithstanding the evident variability in the measurement of particulates, and as highlighted in the discussion of NO_x emissions, constant injection testing of γ-dodecalactone saw combustion commence in the compression stroke. These lower volume conditions are likely to increase pyrolysis in inhomogeneous regions of the fuel-air mixture, relative to CIgn combustion. With a retarded injection timing (CIgn), combustion began at TDC, meaning the cylinder volume is increasing as energy is released and this therefore reduces the likelihood of regions suitable for pyrolysis occurring.

4. Conclusions

Saturated cyclic esters- lactones- were predicted to yield positive combustion characteristics in a compression ignition engine. Therefore, low-carbon number lactones were tested in diesel:butanol blends to obtain their effectiveness as bio-derived diesel fuel extenders. The following conclusions can be drawn from the findings obtained.

- The combustion of the three C6 lactone blends saw a significant increase in ignition delay, relative to fossil diesel, likely due to the low carbon number of the biocomponent, resulting in the ignition quality of the lactone blend being similar to that of an equivalent butanol blend.

- Levels of CO emitted by the C6 lactones were primarily influenced by the extended duration of ignition delay relative to reference diesel. All of the lactones emitted higher levels of CO than reference diesel, likely to be attributable to fuel over-dilution and impingement.

- NO_x emissions followed a general, expected, trend with pHRR; as higher pHRR generally correlates with higher, more sustained temperatures that are necessary for NO_x formation. The butanol blend produced the lowest levels of NO_x due to the poor combustion quality, and therefore low in-cylinder temperatures. γ-decalactone

928   produced the highest pHRR, with a slightly longer ignition delay causing greater

929   premixed combustion, but lower NO_x, than diesel. This was potentially caused by the

930   later onset of pHRR and earlier timing of peak temperature, suggesting more fleeting

931   high temperatures.

932   -   Emissions of particulate mass were reduced relative to reference diesel for all of

933   lactone blends. γ-decalactone registered the lowest mass of all blends, due to the

934   presence of oxygen combined with the higher combustion quality allowing for higher

935   temperatures and therefore enhanced soot oxidation.

936   -   Ultimately, γ-decalactone, despite being blended with butanol, exhibited good

937   combustion characteristics for a diesel fuel. Ignition delay was not increased to the

938   extent that that high amounts of incomplete combustion products were formed, while

939   the lactone oxygen content and higher peak heat release resulted in lower particle

940   mass, and similar particle number, to diesel.

941

942   It was then shown, for the first time, the operation of a diesel engine, without significant

943   modification, using 100% bio-derived lactone fuels. The C10 and C12 lactones tested here

944   can be derived from first generation biomass and, more recently, investigations have outlined

945   potential pathways to obtain the molecules from 2nd generation sources also. From the

946   experimental results presented, the following conclusions can be drawn.

947   -   Ultimately, all of the long-chained lactones showed promising ignition quality,

948   equivalent to or, in the case of γDDL, greater than that of diesel. However, the C12

949   lactones appeared not to alleviate the emissions of particulates, relative to diesel.

950   - NO_x emissions decreased for all lactones compared to diesel, which was explainable

951   by either the magnitude or timing of peak HRR and peak global in-cylinder

952   temperatures; no evidence of an impact of differing physical properties was apparent.

953   -   Combustion of the C10 lactones likely resulted in over dilution and fuel impingement,

954   caused by a relatively long ignition delay, observed by an increase in CO emissions

955   that indicated greater incomplete combustion.

956   -   C10 lactones, due to their slightly lower ignition quality compared to the C12 lactones

957   and diesel, resulted in a lower particle mass and similar number to diesel combustion

958   emissions.

959   The current work outlines a potential novel source of bioderived diesel fuel extenders. The

960   next step to this research is to further understand the fundamental properties of this class of

961   fuels, for example, relating to the long-term storage stability, the heat of vaporisation and the

962   cetane number. It is envisioned that, once production costs of biological pathways have been

963   lowered for this class of molecule, the understanding of the combustion behaviour of lactones

964   is at a stage where they are considered as viable fuel candidates.

965

966

967

968

969

970

971

972

973

974

975

976

977

978

979 **Nomenclature**

980

ATDC	After top-dead centre
BDE	Bond dissociation enthalpy
BTDC	Before top-dead centre
CAD	Crank angle degree
CI	Compression ignition
CIgn	Constant ignition
CInj	Constant injection
CN	Cetane number
CO$_2$	Carbon dioxide
CO	Carbon monoxide
COV	Coefficient of variation
CR	Compression ratio
δDDL	Delta-dodecalactone
δDL	Delta-decalactone
δHL	Delta-hexalactone
εCL	Epsilon-caprolactone
γCL	Gamma-caprolactone
γDDL	Gamma-dodecalactone
γDL	Gamma-decalactone
GHGs	Greenhouse gases
GVL	Gamma-valerolactone
HCs	Hydrocarbons
HRR	Heat release rate
ICE	Internal combustion engine
ICT	In-cylinder temperature

ID	Ignition delay
IMEP	Indicated mean effective pressure
LA	Levulinic acid
NO$_x$	Nitrous oxide
N$_2$	Nitrogen
O$_2$	Oxygen
PAH	Polycyclic aromatic hydrocarbons
pHRR	Peak heat release rate
PM	Particle mass
PN	Particle number
ppm	Parts per million
rpm	Revolutions per minute
SI	Spark ignition
SOC	Start of combustion
SOI	Start of injection
TDC	Top dead centre
UHCs	Unburnt hydrocarbons
µs	Microseconds

981

982

983

984

985

986

987

References

988

989   1.   Independent Statistics and Analysis. US Energy Information Administration. Use of energy
990   explained: Energy use for transportation. (2020).

991   2.   BEIS. *Special feature-Road fuel consumption and the UK motor vehicle fleet Road fuel*
992   *consumption and the UK motor vehicle fleet Background*. (2019).

993   3.   Logan, K. G., Nelson, J. D. & Hastings, A. Low emission vehicle integration: Will National Grid
994   electricity generation mix meet UK net zero? *Proceedings of the Institution of Mechanical*
995   *Engineers, Part A: Journal of Power and Energy* **236**, (2022).

996   4.   Health Organization, W. & Office for Europe, R. *Review of evidence on health aspects of air*
997   *pollution-REVIHAAP Project Technical Report*. (2013).

998   5.   Stevanovic, S. *et al.* Oxidative potential of gas phase combustion emissions - An
999   underestimated and potentially harmful component of air pollution from combustion
1000   processes. *Atmos Environ* **158**, (2017).

1001   6.   Abdel-Shafy, H. I. & Mansour, M. S. M. A review on polycyclic aromatic hydrocarbons: Source,
1002   environmental impact, effect on human health and remediation. *Egyptian Journal of*
1003   *Petroleum* Preprint at https://doi.org/10.1016/j.ejpe.2015.03.011 (2016).

1004   7.   Agarwal, A. K. Biofuels (alcohols and biodiesel) applications as fuels for internal combustion
1005   engines. *Progress in Energy and Combustion Science* Preprint at
1006   https://doi.org/10.1016/j.pecs.2006.08.003 (2007).

1007   8.   García, A., Monsalve-Serrano, J., Martínez-Boggio, S., Rückert Roso, V. & Duarte Souza
1008   Alvarenga Santos, N. Potential of bio-ethanol in different advanced combustion modes for
1009   hybrid passenger vehicles. *Renew Energy* **150**, (2020).

1010   9.   Reşitoɬlu, I. A., Altinişik, K. & Keskin, A. The pollutant emissions from diesel-engine vehicles
1011   and exhaust aftertreatment systems. *Clean Technologies and Environmental Policy* Preprint at
1012   https://doi.org/10.1007/s10098-014-0793-9 (2015).

1013   10.   Zhang, Z. H. & Balasubramanian, R. Investigation of particulate emission characteristics of a
1014   diesel engine fueled with higher alcohols/biodiesel blends. *Appl Energy* (2016)
1015   doi:10.1016/j.apenergy.2015.10.173.

1016   11.   Rakopoulos, D. C., Rakopoulos, C. D., Giakoumis, E. G., Dimaratos, A. M. & Kyritsis, D. C.
1017   Effects of butanol-diesel fuel blends on the performance and emissions of a high-speed di
1018   diesel engine. *Energy Convers Manag* (2010) doi:10.1016/j.enconman.2010.02.032.

1019   12.   Zheng, Z., Wang, X., Yue, L., Liu, H. & Yao, M. Effects of six-carbon alcohols, ethers and
1020   ketones with chain or ring molecular structures on diesel low temperature combustion.
1021   *Energy Convers Manag* (2016) doi:10.1016/j.enconman.2016.07.057.

1022   13.   Osman, M. E. H., Abo-Shady, A. M., Elshobary, M. E., Abd El-Ghafar, M. O. & Abomohra, A. E.
1023   F. Screening of seaweeds for sustainable biofuel recovery through sequential biodiesel and
1024   bioethanol production. *Environmental Science and Pollution Research* **27**, (2020).

1025   14.   Gowthaman, S. & Thangavel, K. Performance, emission and combustion characteristics of a
1026   diesel engine fuelled with diesel/coconut shell oil blends. *Fuel* **322**, (2022).

45

1027   15.   Yesilyurt, M. K. & Aydin, M. Experimental investigation on the performance, combustion and
1028   exhaust emission characteristics of a compression-ignition engine fueled with cottonseed oil
1029   biodiesel/diethyl ether/diesel fuel blends. *Energy Convers Manag* **205**, (2020).

1030   16.   EL-Seesy, A. I. *et al.* Influence of quaternary combinations of biodiesel/methanol/n-
1031   octanol/diethyl ether from waste cooking oil on combustion, emission, and stability aspects
1032   of a diesel engine. *Energy Convers Manag* **240**, (2021).

1033   17.   Frost, J., Hellier, P. & Ladommatos, N. A systematic study into the effect of lignocellulose-
1034   derived biofuels on the combustion and emissions of fossil diesel blends in a compression
1035   ignition engine. *Fuel* **313**, (2022).

1036   18.   Srinivasamurthy, V. S. T., Böttcher, D., Engel, J., Kara, S. & Bornscheuer, U. T. A whole-cell
1037   process for the production of ε-caprolactone in aqueous media. *Process Biochemistry* (2020)
1038   doi:10.1016/j.procbio.2019.10.009.

1039   19.   Buntara, T. *et al.* Caprolactam from renewable resources: Catalytic conversion of 5-
1040   hydroxymethylfurfural into caprolactone. *Angewandte Chemie - International Edition* (2011)
1041   doi:10.1002/anie.201102156.

1042   20.   Gupta, S., Arora, R., Sinha, N., Alam, M. I. & Haider, M. A. Mechanistic insights into the ring-
1043   opening of biomass derived lactones. *RSC Adv* (2016) doi:10.1039/c5ra22832h.

1044   21.   Dubal, S. A., Tilkari, Y. P., Momin, S. A. & Borkar, I. v. Biotechnological routes in flavour
1045   industries. *Advanced Biotech* **14**, (2008).

1046   22.   Neto, R. S., Pastore, G. M. & Macedo, G. A. Biocatalysis and Biotransformation Producing γ-
1047   Decalactone. *J Food Sci* (2006) doi:10.1111/j.1365-2621.2004.tb09914.x.

1048   23.   Tahara, S., Fujiwara, K. & Mizutani, J. Neutral constituents of volatiles in cultured broth of
1049   sporobolomyces odorus. *Agric Biol Chem* (1973) doi:10.1271/bbb1961.37.2855.

1050   24.   Schrader, J., Etschmann, M. M. W., Sell, D., Hilmer, J. M. & Rabenhorst, J. Applied biocatalysis
1051   for the synthesis of natural flavour compounds - Current industrial processes and future
1052   prospects. *Biotechnology Letters* Preprint at
1053   https://doi.org/10.1023/B:BILE.0000019576.80594.0e (2004).

1054   25.   Braga, A. & Belo, I. Biotechnological production of γ-decalactone, a peach like aroma, by
1055   Yarrowia lipolytica. *World Journal of Microbiology and Biotechnology* Preprint at
1056   https://doi.org/10.1007/s11274-016-2116-2 (2016).

1057   26.   An, J. U., Joo, Y. C. & Oh, D. K. New biotransformation process for production of the fragrant
1058   compound γ-dodecalactone from 10-hydroxystearate by permeabilized waltomyces lipofer
1059   cells. *Appl Environ Microbiol* (2013) doi:10.1128/AEM.02602-12.

1060   27.   Jo, Y. S., An, J. U. & Oh, D. K. γ-Dodecelactone production from safflower oil via 10-hydroxy-
1061   12(z)-octadecenoic acid intermediate by whole cells of candida boidinii and
1062   stenotrophomonas nitritireducens. *J Agric Food Chem* (2014) doi:10.1021/jf501081z.

1063   28.   Serra, S. & De Simeis, D. Use of Lactobacillus rhamnosus (ATCC 53103) as whole-cell
1064   biocatalyst for the regio- and stereoselective hydration of oleic, linoleic, and linolenic acid.
1065   *Catalysts* (2018) doi:10.3390/catal8030109.

1066 29.   Ha, L., Mao, J., Zhou, J., Zhang, Z. C. & Zhang, S. Skeletal isomerization of unsaturated fatty
1067   acids on Beta zeolites: Effects of calcination temperature and additives. *Appl Catal A Gen*
1068   (2009) doi:10.1016/j.apcata.2008.12.018.

1069 30.   Corma, A., Iborra, S., Mifsud, M., Renz, M. & Susarte, M. A new environmentally benign
1070   catalytic process for the asymmetric synthesis of lactones: Synthesis of the flavouring δ-
1071   decalactone molecule. *Adv Synth Catal* (2004) doi:10.1002/adsc.200303234.

1072 31.   Alam, M. I., Khan, T. S. & Haider, M. A. Alternate Biobased Route to Produce Î-Decalactone:
1073   Elucidating the Role of Solvent and Hydrogen Evolution in Catalytic Transfer Hydrogenation.
1074   *ACS Sustain Chem Eng* (2019) doi:10.1021/acssuschemeng.8b05014.

1075 32.   Bohre, A., Dutta, S., Saha, B. & Abu-Omar, M. M. Upgrading Furfurals to Drop-in Biofuels: An
1076   Overview. *ACS Sustainable Chemistry and Engineering* Preprint at
1077   https://doi.org/10.1021/acssuschemeng.5b00271 (2015).

1078 33.   Raspolli Galletti, A. M. *et al.* From giant reed to levulinic acid and gamma-valerolactone: A
1079   high yield catalytic route to valeric biofuels. *Appl Energy* (2013)
1080   doi:10.1016/j.apenergy.2012.05.061.

1081 34.   Bereczky, Á., Lukács, K., Farkas, M. & Dóbé, S. Effect of <i>γ</i>-Valerolactone
1082   Blending on Engine Performance, Combustion Characteristics and Exhaust Emissions in a
1083   Diesel Engine. *Natural Resources* (2014) doi:10.4236/nr.2014.55017.

1084 35.   Horváth, I. T., Mehdi, H., Fábos, V., Boda, L. & Mika, L. T. γ-Valerolactone—a sustainable
1085   liquid for energy and carbon-based chemicals. *Green Chemistry* (2008)
1086   doi:10.1039/b712863k.

1087 36.   Makhubela, B. C. E. & Darkwa, J. The Role of Noble Metal Catalysts in Conversion of Biomass
1088   and Bio-derived Intermediates to Fuels and Chemicals. *Johnson Matthey Technology Review*
1089   (2018) doi:10.1595/205651317X696261.

1090 37.   Gschwend, D., Soltic, P., Wokaun, A. & Vogel, F. Review and Performance Evaluation of Fifty
1091   Alternative Liquid Fuels for Spark-Ignition Engines. *Energy and Fuels* (2019)
1092   doi:10.1021/acs.energyfuels.8b02910.

1093 38.   Liang, X., Duan, Y., Fan, Y., Huang, Z. & Han, D. Influences of C5 esters addition on anti-knock
1094   and auto-ignition tendency of a gasoline surrogate fuel. *International Journal of Engine
1095   Research* (2021) doi:10.1177/14680874211030898.

1096 39.   Chen, Z., Wang, Z., Lei, T. & Gupta, A. K. Physical-Chemical Properties and Engine
1097   Performance of Blends of Biofuels with Gasoline. *J Biobased Mater Bioenergy* **15**, (2021).

1098 40.   Rajesh Kumar, B. & Saravanan, S. Use of higher alcohol biofuels in diesel engines: A review.
1099   *Renewable and Sustainable Energy Reviews* Preprint at
1100   https://doi.org/10.1016/j.rser.2016.01.085 (2016).

1101 41.   Vinod Babu, V. B. M., Madhu Murthy, M. M. K. & Amba Prasad Rao, G. Butanol and pentanol:
1102   The promising biofuels for CI engines – A review. *Renewable and Sustainable Energy Reviews*
1103   Preprint at https://doi.org/10.1016/j.rser.2017.05.038 (2017).

1104 42.   Yang, Miao; Wang, Zhiwei; Lei, Tingzhou; Lin, Lu; He, Xiaofeng; Qi, Tian; Xin, Xiaofei; Li, Zijie;
1105   Shi, J. Influence of Gamma-Valerolactone-n-Butanol-Diesel Blends on Physicochemical

1106   Characteristics and Emissions of a Diesel Engine. *J Biobased Mater Bioenergy* **11**, 66–72
1107   (2017).

1108 43.   Yilmaz, N., Vigil, F. M., Benalil, K., Davis, S. M. & Calva, A. Effect of biodiesel-butanol fuel
1109   blends on emissions and performance characteristics of a diesel engine. *Fuel* (2014)
1110   doi:10.1016/j.fuel.2014.06.022.

1111 44.   Lapuerta, M., Hernández, J. J., Fernández-Rodríguez, D. & Cova-Bonillo, A. Autoignition of
1112   blends of n-butanol and ethanol with diesel or biodiesel fuels in a constant-volume
1113   combustion chamber. *Energy* (2017) doi:10.1016/j.energy.2016.10.090.

1114 45.   Zhang, P. *et al.* Spray, atomization and combustion characteristics of oxygenated fuels in a
1115   constant volume bomb: A review. *Journal of Traffic and Transportation Engineering (English*
1116   *Edition)* Preprint at https://doi.org/10.1016/j.jtte.2020.05.001 (2020).

1117 46.   Kumbár, V. & Skřivánek, A. Temperature dependence viscosity and density of different
1118   biodiesel blends. *Acta Universitatis Agriculturae et Silviculturae Mendelianae Brunensis* **63**,
1119   (2015).

1120 47.   Zigan, L., Schmitz, I., Flügel, A., Wensing, M. & Leipertz, A. Structure of evaporating single-
1121   and multicomponent fuel sprays for 2nd generation gasoline direct injection. *Fuel* **90**, (2011).

1122 48.   Ahmed, M. B. & Mekonen, M. W. Effects of Injector Nozzle Number of Holes and Fuel
1123   Injection Pressures on the Diesel Engine Characteristics Operated with Waste Cooking Oil
1124   Biodiesel Blends. *Fuels* **3**, 275–294 (2022).

1125 49.   Brown, H. C., Brewster, J. H. & Shechter, H. An Interpretation of the Chemical Behavior of
1126   Five- and Six-membered Ring Compounds. *J Am Chem Soc* (1954) doi:10.1021/ja01631a041.

1127 50.   Hellier, P., Ladommatos, N. & Yusaf, T. The influence of straight vegetable oil fatty acid
1128   composition on compression ignition combustion and emissions. *Fuel* (2015)
1129   doi:10.1016/j.fuel.2014.11.021.

1130 51.   Omidvarborna, H., Kumar, A. & Kim, D. S. Variation of diesel soot characteristics by different
1131   types and blends of biodiesel in a laboratory combustion chamber. *Science of the Total*
1132   *Environment* (2016) doi:10.1016/j.scitotenv.2015.11.076.

1133 52.   Zhang, Z. H. & Balasubramanian, R. Effects of oxygenated fuel blends on the composition of
1134   size-segregated engine-out diesel particulate emissions and on the toxicity of quasi-ultrafine
1135   particles. *Fuel* (2018) doi:10.1016/j.fuel.2017.10.097.

1136 53.   Eveleigh, A., Ladommatos, N., Hellier, P. & Jourdan, A. L. An investigation into the conversion
1137   of specific carbon atoms in oleic acid and methyl oleate to particulate matter in a diesel
1138   engine and tube reactor. *Fuel* (2015) doi:10.1016/j.fuel.2015.03.037.

1139 54.   Hellier, P., Talibi, M., Eveleigh, A. & Ladommatos, N. An overview of the effects of fuel
1140   molecular structure on the combustion and emissions characteristics of compression ignition
1141   engines. *Proceedings of the Institution of Mechanical Engineers, Part D: Journal of Automobile*
1142   *Engineering* (2017) doi:10.1177/0954407016687453.

1143 55.   Jacobson, R. S., Korte, A. R., Vertes, A. & Miller, J. H. The Molecular Composition of Soot.
1144   *Angewandte Chemie* (2020) doi:10.1002/ange.201914115.

1145   56.   Salamanca, M. *et al.* The impact of cyclic fuels on the formation and structure of soot.
1146   *Combust Flame* (2020) doi:10.1016/j.combustflame.2020.04.026.

1147   57.   Commodo, M. *et al.* On the early stages of soot formation: Molecular structure elucidation by
1148   high-resolution atomic force microscopy. *Combust Flame* (2019)
1149   doi:10.1016/j.combustflame.2019.03.042.

1150   58.   Svensson, K. I., Richards, M. J., MacKrory, A. J. & Tree, D. R. Fuel composition and molecular
1151   structure effects on soot formation in direct-injection flames under diesel engine conditions.
1152   in *SAE Technical Papers* (2005). doi:10.4271/2005-01-0381.

1153   59.   Koivisto, E., Ladommatos, N. & Gold, M. Systematic study of the effect of the hydroxyl
1154   functional group in alcohol molecules on compression ignition and exhaust gas emissions.
1155   *Fuel* (2015) doi:10.1016/j.fuel.2015.03.042.

1156   60.   Xin, L. *et al.* Thermal decomposition mechanism of some hydrocarbons by ReaxFF-based
1157   molecular dynamics and density functional theory study. *Fuel* (2020)
1158   doi:10.1016/j.fuel.2020.117885.

1159

1160

1161

1162

1163

1164

1165

1166

1167

1168

1169

1170

1171

1172

1173

1174

1175

1176

1177